Memo

To:	CCB
From:	Jin Wang and Keith McLaughlin
Date:	January 19, 1999
Subject:	Global Slowness-Azimuth Station Calibrations (GSASC) for the IMS network
Sponsor:	Robert North
CC:	Hans Israelsson

Abstract

The Slowness-Azimuth Station Corrections (SASC) have been implemented in the PIDC since April, 1998 (Bondar, 1998). Currently, all seismic arrays and primary 3C stations have SASCs except ABKT, BRAR, CPUP, KBZ, NOA, NRIS, PDY, ROSC and ZAL. The SASCs were designed to correct slowness and azimuth in predefined bins. The SASCs have successful reduced the slowness and azimuth residuals in the corrected bins. However, for detections outside of corrected bins, observations would not been corrected. Besides, the current SASCs were derived from teleseismic data so that no regional seismic phases would be corrected.

In this proposal, a systematic tuning approach is developed for improving slowness and azimuth determinations at three-component stations. It employs a station-specific parameter (***polar-alpha***) to estimate slowness, and a Station-specific Equivalent Mis-orientation Angle (***SEMA***) to improve azimuth estimation. This approach is based on the physical meaning of the slowness formula for 3C stations, polarization property of 3C waveforms, and the empirical data performance. Since this tuning method is applied to all detections for each 3C station, it could be called Global Slowness Azimuth Station Calibration (GSASC) compared with the SASC. The GSASC is a very simple yet effective approach with clear physical meanings. It is a first-order correction for 3C stations while the SASC is fine-tune correction in the pre-defined slowness-azimuth bins. Using the GSASC approach, a set of new values of the parameter, ***polar-alpha***, and the equivalent mis-orientation angles (***SEMA***) for primary 3C stations have been derived. To incorporate with GSASC implementations, which would remove the systematic bias in slowness and azimuth estimations, the existing SASC files have been re-estimated accordingly. At the same time, the SASCs for arrays have been updated with more empirical data and an extended grid that includes regional and local seismic slownesses. On-line and off line testing with these new values show

that improvement of slowness and azimuth estimations has been achieved for most of the tested 3C stations.

Statement of Objective

The objective of this proposal is to improve the accuracy of slowness and azimuth estimations for IMS network. Particularly, this proposal aims to remove systematic bias of the observed slowness and azimuth values because of the un-tuned default parameter in slowness estimation and the equivalent mis-orientation at primary 3C stations.

Summary of Proposed Change

This proposal recommends following changes:

1) Replace the current default value (0.3) of the parameter ***polar-alpha***, which is defined in the corresponding files *$(STA)-polor.par* in the directory */cmss/config/app_config/DFX/polar*, with the proposed station-specific value for the 3C stations listed in Table 1.

2) The SEMAs of stations BGCA, DBIC, MNV, NRIS, PLCA, STKA, VNDA, and ZAL of Table 1 can be incorporated into several ways in operations. We recommend that a new table, being a copy of the existing ***sitechan*** table, is added and then the attribute '*hang*' of the existing ***sitechan*** table is updated in accordance with Table 1 for these eight stations.

This means that the added ***sitechan*** table (called e.g., ***ndc_sitechan***) would store 'official' information on instrument orientation provided by NDCs, whereas the existing or 'operational' table would contain corrected information consistent with actual data. ***SEMA*** changes in the future would be made in the ***sitechan*** tables and changes provided by NDCs would be made in the 'official' sitechan table and, as appropriate, in the existing operational ***sitechan*** table.

DFX processing based on such an operational table would fully draw upon all the ***SEMA*** corrections in Table 1 for azimuth estimation which affects 8 or half of the primary 3C stations, and also ensure that polarization attributes, used for phase identification, would be determined in a manner consistent with the azimuth estimation. ***SEMA*** corrections can also be easily be incorporated for auxiliary stations in the future. An operational table, however, comes at the price of additional book-keeping and maintenance of the 'ndc table' by operations and station quality control.

From the point of view of performance other alternatives to implement the ***SEMA***s of Table 1 in operations are less satisfactory as azimuth and polarization attribute estimates would neither be determined consistently nor completely corrected for; incorporation of SEMAs in the SASC files will not be correct for stations NRIS and ZAL and LR phases and polarization attributes would not be determined from correct orientations; updating attributes ***arrival***.*azimuth* and ***detection***.*seaz* after DFX processing with SQL scripts would not give consistently processed polarization parameters.

3) Update the SASC files of 3C stations to avoid duplicate corrections in the SASC bins; the updated SASC files are derived from data corrected for global slowness-azimuth station calibrations.

4) Update the SASC files of arrays with more training data and a new grid file which includes regional and local slownesses.

Expected Benefits

The global slowness azimuth station calibrations proposed here and the related new SASCs will significantly improve slowness and azimuth estimation for primary 3C stations. The new SASCs of arrays have more correction bins so that more detections are expected to be corrected. Phase identification, association and locations should be improved for the IMS network.

Possible Risks and Dependencies

Although the proposed new values have been tested with 20-day on-line data, the impact of the improved slowness and azimuth determination on final event formation has not been evaluated. There would be a small impact on the event formation where slowness and azimuth features are used. *Hang* value changes require resolution of SMR CMR-472 which will fix the correct rotation of horizontal components in *DFX*.

The *DFX* function */cmss/rel/src/automatic/src/DFX/libsrc/libthreec/threec.c* must be modified by changing:

```
hrot = -1.0 * wn->hang;
```

to:

```
hrot = 1.0 * wn->hang.
```

This modification will rotate waveforms correctly.

Summary of Testing

The recommendations are based on the evaluation of slowness and azimuth determination and testing. The evaluation and testing results are summarized as the following:

1) The new values of slowness parameter, ***polar-alpha***, which are derived from the relation between the predicated and observed slowness for each primary 3C stations, will reduce slowness residuals overall and move the peaks of the histograms toward zero.

2) The station-specific equivalent mis-orientation angles, ***SEMA***, which are derived from the azimuth residuals, will reduce azimuth residuals overall and move the peaks of the histograms toward zero.

3) Special analyses have been applied to the stations NRIS and ZAL. The related slowness and azimuth correction formulas derived from the recent data will correct the current azimuth and slowness anomaly.

4) On-line testing of 20 days for these new values of ***polar-alpha*** and the ***SEMA*** calibrations shows that the expected improvements on removing bias of slowness and residuals have been achieved in most of the tested stations.

5) Off-line testing for the incorporation of GSSCs and SASCs has been tested. It shows both files can work properly and the expected improvement has been achieved.

Plan and Schedule for Implementation

We recommend implementation as soon as possible.

To implement this proposal, we need to do followings:

1) Modify the parameter ***polar-alpha*** in files *$(STA)-polar.par* in the directory */cmss/config/app_config/DFX/polar*, based on Table 1.

2) Create a table called ***ndc_sitechan*** that is the copy of existing database table ***sitechan.***

3) Update the database attribute ***sitechan.****hand* for stations BGCA, DBIC, MNV, NRIS, PLCA, VNDA and ZAL based on Table 1. This is conditioned upon resolution of SMR CMR-472.

4) Copy the updated SASC files *sasc.$(STA)* in the directory */home/jinwang/NewSASC* to */cmss/config/earth_specs/SASC*.

Costs and Resources Required for Implementation

It will take about one hour of an operator's time to modify the related database attributes and parameter files. Resolution SMR CMR-472 is unknown at this time. A patch to *DFX* function *threec.c* must be released and installed.

Acknowledgments

We are grateful to Istvan Bondar for his invaluable work in SASC software, for Jianjun Zhang for his kindly help to test the proposed values, and to Hans Israelsson and Richard Stead for their comments and suggestions.

Table 1: Recommended Station-dependent Slowness Parameters (default=0.3 s/km) and the new hang values based on Equivalent Mis-orientation Angles (measured clockwise from the North). The hang values in brackets are current values not need changes

Station	**new *polar-alpha* (sec/km)**	***New sitechan.hang***		***SEMA* *(Azi = obs_azi + SEMA)***
		N	***E***	
BDFB	0.3501	(0)	(90)	0
BGCA	0.2742	10	100	10
BJT	0.4407	(0)	(90)	0
BOSA	0.2831	(0)	(90)	0
CPUP	0.2737	(335)	(65)	0
DBIC	0.2676	19	109	19
HIA	0.3358	(0)	(90)	0
MAW	0.2408	(0)	(90)	0
MNV	0.4443	348	78	-12
NRIS	0.3983	314	224	AZI = 270 - obs_azi + 44
PLCA	0.2686	5	95	5
SCHQ	0.2527	(0)	(90)	(21)
STKA	0.3026	354	84	-6
ULM	0.2890	(0)	(90)	0
VNDA	0.2878	8	98	8
ZAL	0.3159	295	205	AZI = 270 - obs_azi + 25

Appendix

A.1 Evaluation of slowness and azimuth estimations at 3C primary stations

To evaluate performance of slowness and azimuth estimations at primary 3C stations, fifteen months of data (01/01/97 to 03/31/98) were analyzed. The relationship patterns between the observed and predicted feature (slowness or azimuth) values, and histograms of observation residuals have been generated using the associated phases in REB with signal-to-noise ratio being equal or greater than 8. Ideally, the relation between the observed values (***SEL3.arrival***.*slow* or ***SEL3.arrival***.*azimuth*) and the theoretical values (***REB.arrival***.*slow* - ***REB.assoc***.*slores* for predicted slowness or ***REB.assoc***.*seaz* for predicted azimuth) should be along a straight line with a slope of 1. At the same time, the peak of the histogram of residuals should be centered at zero. In reality, however, there is a systematic bias in observations for many stations. Figure 1 shows the relationship between the observed and theoretical features at station DBIC. There is a 19 degrees offset for the peak of the histogram of azimuth residuals as shown in the upper-right subplot in Figure 1. We also can see that the observed slownesses are systematically smaller than the theoretical slownesses from the lower-left subplot in the figure. The median of slowness residuals is 0.61 sec/deg and the peak of histogram of slowness residuals has also an offset. All statistical results for primary 3C stations are given in Figures 8-22 and summarized in Table 2. For station NRIS and ZAL, 11 months of recent data (1/1/1998 - 11/30/98) are used in the statistics because these tri-axial stations from time to time suffer inconsistent station problems (Wang and Stead, 1998). The stations have been consistent for at least in the 11 months.

The Slowness-Azimuth Station Corrections (SASC) have been implemented in the PIDC since April, 1998 (Bondar, 1998). Currently, all seismic arrays and primary 3C stations have SASCs except ABKT, BRAR, CPUP, KBZ, NOA, NRIS, PDY, ROSC and ZAL. The SASCs were designed to correct slowness and azimuth in predefined bins. The SASCs have successful reduced the slowness and azimuth residuals in the corrected bins. However, for detections outside of corrected bins, observations would not been corrected. Besides, the current SASCs were derived from teleseismic data so that no regional seismic phases would be corrected.

Previous investigations found the database entries ***sitechan***.*hang* for N and E components were switched for station CPUP. These values have been recently fixed in the database. This investigation uncovered further problems with *DFX* function *threec.c* which is incorrectly applying ***sitechan***.*hang* to horizontal components when hang values are not 0 or 90 degrees.

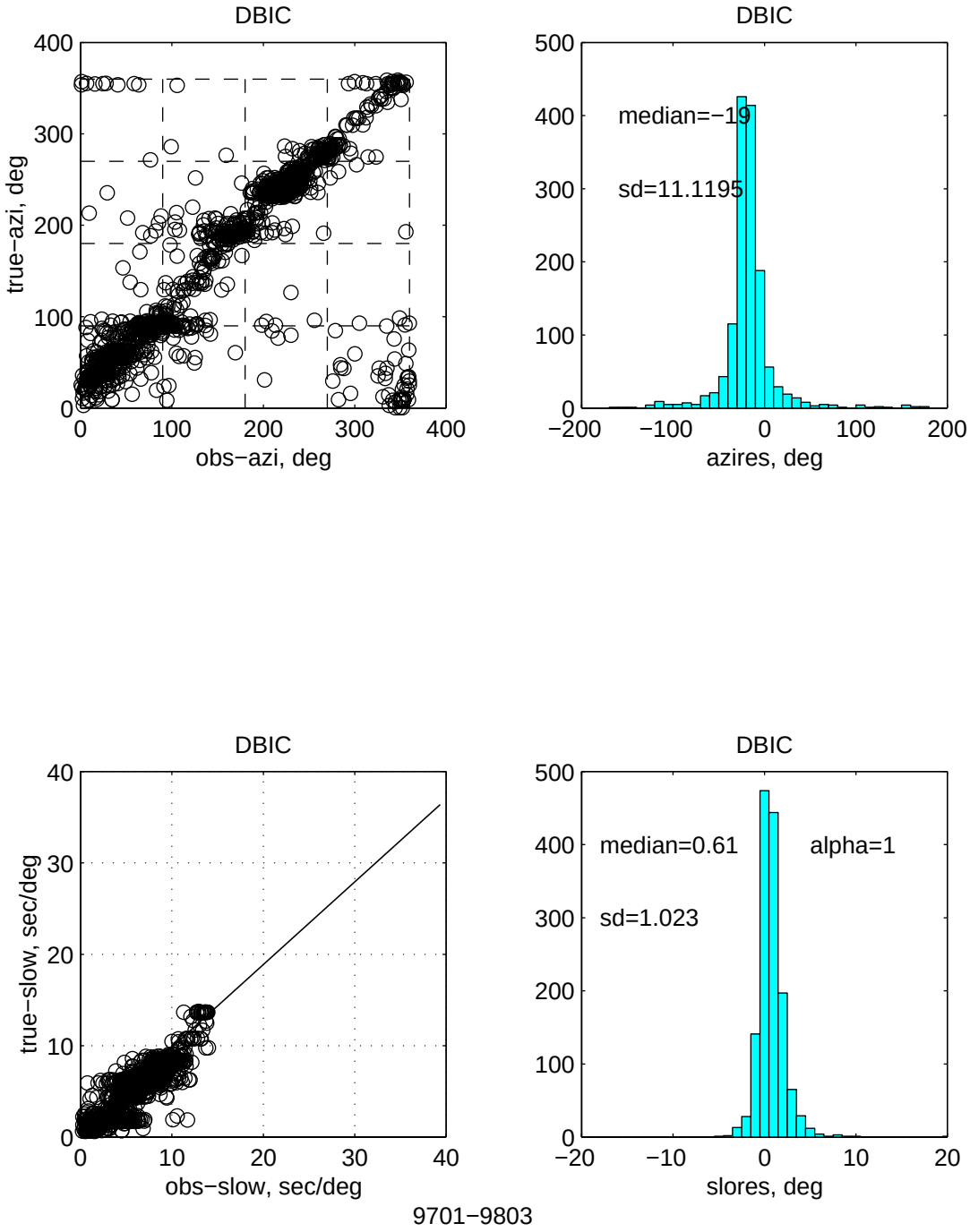

Figure 1. Performance of slowness and azimuth estimations at station DBIC. The upper-left subplot is the relations between the azimuth observations and the predicted azimuth values. The lower-left subplot is the relations between the slowness observations and the predicted slowness values. The upper-right subplot is the histogram of the azimuth residuals. The lower-right subplot is the histogram of the slowness residuals. It shows that there is a bias in the azimuth and the slowness determination.

Table 2: Statistics of azimuth and slowness residuals for primary 3C stations at the PIDC

Station	Number of phases (SNR>=8.0)	Slowness residuals (sec/deg)		Azimuth residuals (deg)	
		Median	Std	Median	Std
BDFB	1429	-0.95	1.47	-1.0	14.2
BGCA	2310	0.46	0.90	-9.9	10.7
BJT	1084	-2.56	2.05	-4.4	23.1
BOSA	1045	0.29	1.17	1.4	13.8
CPUP	670	0.64	1.23	6.3	167.6
DBIC	1518	0.61	1.02	-19	11.1
HIA	1578	-0.83	1.28	3.4	10.2
LPAZ	2177	-1.27	3.08	1.6	21.7
MAW	873	1.32	1.29	-3.6	12.8
MNV	1045	-1.99	1.69	11.6	21.9
NRIS	622	-1.59	1.42	23.8	93.7
PLCA	1285	0.68	1.39	-4.5	13.8
SCHQ	964	1.13	1.55	-20.9	15.6
STKA	3709	-0.06	1.25	5.7	11.4
ULM	1350	0.25	0.83	-0.7	6.2
VNDA	1562	0.28	1.20	-8.3	15.2
ZAL	1953	-0.34	1.41	37.7	83.3

A.2 Global Slowness Station Calibration for 3C stations

For 3C stations, the slowness is estimated in the software *DFX* by the formula:

$$\text{slowness} = (\boldsymbol{polar–alpha}) \bullet \sin\left(\frac{inc}{2}\right) \text{ sec/km,} \qquad (1)$$

where *inc* is the apparent incidence angle determined from the polarization analysis and saved in the database as ***SEL3.arrival****.ema*. The ***polar-alpha*** is a parameter to convert the apparent incidence angle to slowness. Currently, all 3C stations at PIDC use a default value 0.30 for the ***polar-alpha***. To find a right approach for slowness estimations, a simple discussion on the physical meaning of this parameter is given below.

By definition:
$$\text{slowness} = \frac{\sin(INC)}{\mathrm{V}} \qquad (2)$$

where *INC* is the true incidence angle, and V is the phase velocity of the incident seismic wave at ground surface.

For free surface movement with P-waves incidence from the underneath, the relation of **true** incident angle *INC* and **apparent** incident angle *inc* is given by (Bullen, pp128-130,1963):

$$2(\sin(INC))^2 = \left(\frac{\mathrm{V_p}}{\mathrm{V_s}}\right)^2 (1 - \cos(inc)) \qquad (3)$$

where Vp, Vs are the relevant P, S velocities.

Substitute relation (3) into (2) and use the trigonometric relation, $\sin\frac{\theta}{2} = \sqrt{\frac{(1-\cos\theta)}{2}}$, we can get:

$$\text{slowness} = \frac{1}{\mathrm{V_s}} \sin\left(\frac{inc}{2}\right) \qquad (4)$$

Comparing equation (4) with (1), we get the relation:

$$\boldsymbol{polar–alpha} = \frac{1}{\mathrm{V_s}}, \qquad (5)$$

This relation shows the parameter ***polar-alpha*** corresponds to the reciprocal of shear-wave

velocity at the ground surface for each station. That is to say, generating station-specific ***polar-alpha*** values will reflect the local geological property of each station.

Since ***polar-alpha*** is the reciprocal of shear-wave velocity at the ground surface, which is a station-dependent parameter, it is straight-forward to tune the parameter ***polar-alpha*** for each station to improve slowness determination.

The method we proposed to determine station-specific parameter ***polar-alpha*** can be described as the following steps:

1) Define the relation between observed and predicated slowness by

$$slowness_{predicated} = alpha * slowness_{observed}, \quad (6)$$

as shown in the lower-left subplot in Figure 1.

2) Derive the *alpha* (slope of the regression line fit to the relation between predicted and observed slowness) in the least square sense.

3) Determine the station-specific parameter ***polar-alpha*** by a simple multiplication:

$$\textbf{\textit{polar-alpha}}_{new} = alpha * \textbf{\textit{polar-alpha}}_{current}, \quad (7)$$

where $\textbf{\textit{polar-alpha}}_{current}$ is the value being used at each station, which is 0.30 for all 3C stations currently. For example, the *alpha* for station DBIC is 0.8921, so the 'best-fit' slowness parameter ***polar-alpha*** can be estimated by 0.8921 * 0.30 = 0.2676. A set of ***polar-alpha***'s for primary 3C stations have been derived using this approach from 15-months data (01/01/1997 - 03/31/1998) except for stations NZRIS and ZAL which use more recent data (01/01/1998 - 11/30/98). Table 3 lists all derived station-specific ***polar-alpha*** and the corresponding shear-wave velocities.

Using the derived polar-alpha to corrected the observed slowness, the systematic slowness bias would be removed. The lower two subplots of Figure 2 show that the corrected slowness now have one-to-one relations with some scatter, and the peak of the slowness residual histogram has moved toward zero.

This approach is a very simple yet effective method with a clear physical meaning to improve overall slowness determination. This approach could be called Global Slowness Station Calibration (GSSC) for 3C stations compared with the bin Slowness-Azimuth Station Correction (SASC) proposed by Bondar (1998).

Table 3: Station-dependent slowness parameters and inferred shear-wave velocities

Station	*polar-alpha* (s/km)	Vs (km/s)
BDFB	0.3501	2.86
BGCA	0.2742	3.65
BJT	0.4407	2.27
BOSA	0.2831	3.53
CPUP	0.2737	3.65
DBIC	0.2676	3.74
HIA	0.3358	2.98
LPAZ	0.3772	2.65
MAW	0.2408	4.15
MNV	0.4443	2.25
NRIS	0.3983	2.51
PLCA	0.2686	3.72
SCHQ	0.2527	3.96
STKA	0.3026	3.30
ULM	0.2890	3.46
VNDA	0.2878	3.47
ZAL	0.3159	3.17

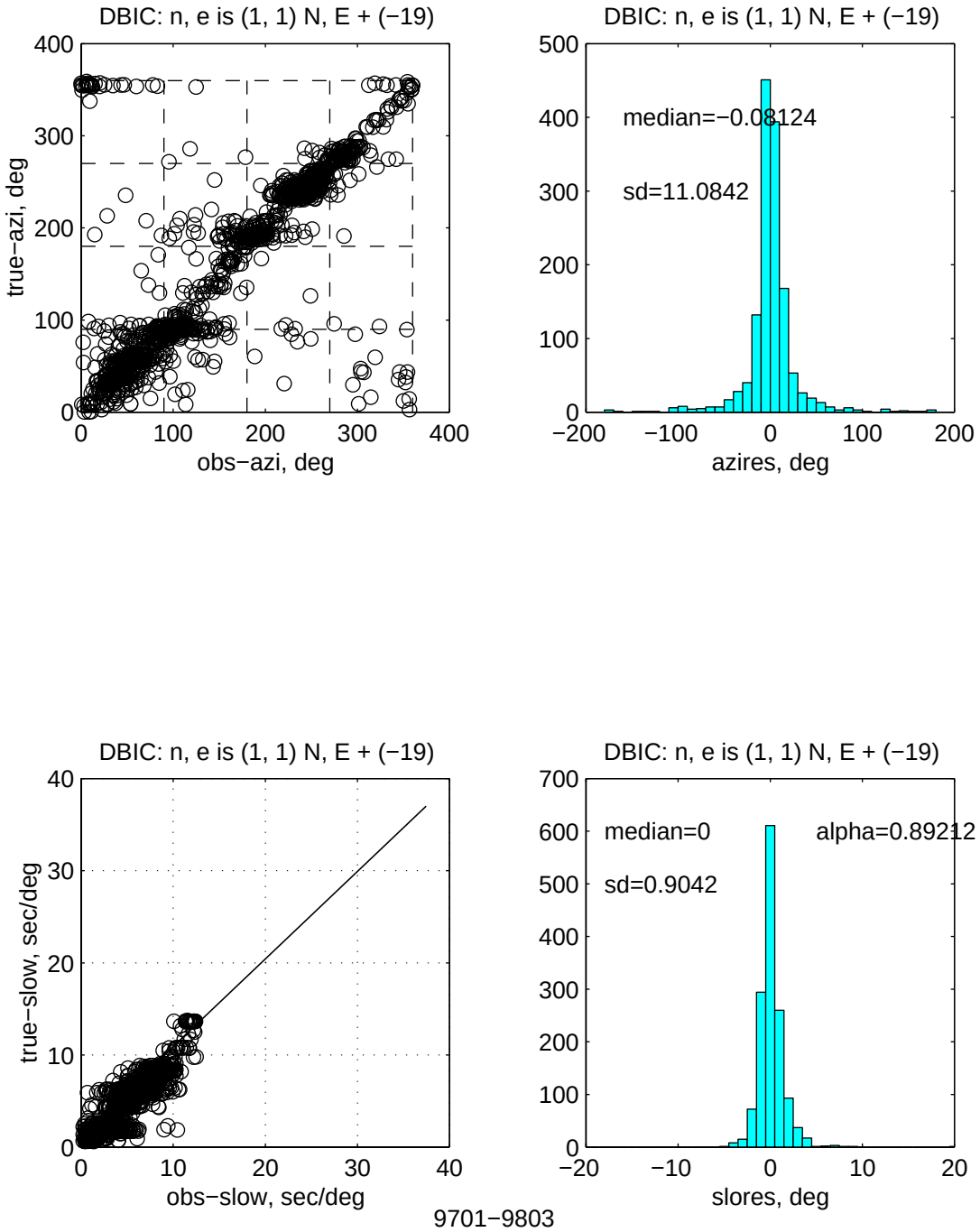

Figure 2. The GSASC performance for DBIC. The upper-left subplot is the relations between the corrected azimuth observations and the predicted azimuth values. The lower-left subplot is the relations between the corrected slowness observations and the predicted slowness values. The upper-right subplot is the histogram of the corrected azimuth residuals. The lower-right subplot is the histogram of the corrected slowness residuals. Compared with Figure 1, the GSASC has removed the systematic slowness and azimuth biases effectively.

A.3 Global Azimuth Station Calibration for 3C stations

An algorithm has been developed to infer the channel status of 3C stations using the observed and predicted azimuth and slowness values (Wang and Stead, 1998). The algorithm has successfully found some stations whose channels were dead or swapped. This algorithm can also infer the mis-orientation angle of each sensor system by searching a rotation angle so that both the sum of absolute value of azimuth residuals and the standard deviation of azimuth residuals are minimum at the same time. However, since many factors would affect azimuth estimation, such as signal-to-noise ratio of detections, seismic ray-path and local geology, the rotation angle inferred from the observation data is not necessarlly the true orientation error of the instrument. We call this angle the Station-specific Equivalent Mis-orientation Angle (***SEMA***). Table 4 lists all inferred ***SEMA*** values and channel anomaly status at some stations. The angle is positive measured clockwise from the North direction.

These ***SEMA***s can be used to correct the orientations defined in the database by the attribute ***sitechan***.*hang*. This correction will affect all data processing modules which involve polarization features. To be conservative, we only recommend updating those stations whose ***SEMA*** is significant biased from zero. Here we adopt 5 degrees as the threshold. Using this criterion, stations BGCA, DBIC, MNV, NRIS, PLCA, SCHQ, STKA, VNDA and ZAL have significant orientation error and should be corrected systematically. To further verify the angles inferred from body wave detections, the performance of another independent azimuth estimation from surface-wave detections were analyzed for some stations. Column 3 of Table 4 shows the results. Comparing Columns 2 and 4, we found that LR surface-wave results partially support the results from body-waves. Considering the results of body waves were derived from a larger number of detections with high SNR while results of surface waves detections from smaller data sets and no SNR selection available, we think the derived ***SEMA***s are reliable for these 3C stations.

The advantage of this Global Azimuth Station Calibration (GASC) approach, which updates database attributes, is simple and consistent. The disadvantage of this approach, however, is the inferred ***SEMA*** is not necessarily the true orientation error of the instrument so that this correction might mislead users of the database.

If we choose not to correct the ***sitechan***.*hang* values it is still possible to correct slowness vectors by the estimated ***SEMA***. As an alternate option, the GASC can be achieved by updating ***arrival***.*azimuth* and ***detection***.*seaz* of all detections after every *DFX* processing using a SQL script. The disadvantage of this approach is that the correction may not be complete and the working load of the system will be increased.

Due to the horizontal components of tri-axial stations are transformed from the three internal channels, which would have different channel anomaly status time by time, it is not proper to correct azimuths by changing ***sitechan***.*hang* at these stations. NRIS and ZAL can be fixed approximately with the formulas:

AZI = 270 - obs_azi + 44 for NRIS

and AZI = 270 - obs_azi + 25 for ZAL.

Station PDY has been found to have a broken internal component and no degree of SASC or SEMA will fix it. PDY is scheduled for upgrade to an array in early 1999 and perhaps will be fixed at that time.

Previous investigations found the database entries ***sitechan***.*hang* for N and E components were switched for station CPUP. These values have been recently fixed in the database. This investigation uncovered further problems with *DFX* function *threec.c* which is incorrectly applying ***sitechan***.*hang* to horizontal components when hang values are not 0 or 90 degrees.

Table 4: Station-dependent *SEMAs* inferred from body waves and surface waves

Station	***SEMA (±σ)***	**Channel status**	***SEMA* (±σ) by surface waves**
BDFB	1 (0.4)		
BGCA	10 (0.2)		10 (4.6)
BJT	4 (0.7)		
BOSA	-1 (0.3)		
CPUP	-2	[n e] = [E N]	
DBIC	19 (0.3)		19 (3.0)
HIA	-3 (0.3)		
LPAZ	-2 (0.5)		
MAW	4 (0.4)		
MNV	-12 (0.7)		5 (3.1)
NRIS	44	[n e] = - [E N]	
PLCA	5 (0.4)		1 (3.2)
SCHQ	21 (0.5)		18 (5.4)
STKA	-6 (0.2)		-1 (1.8)
ULM	1 (0.2)		
VNDA	8 (0.4)		-4 (3.1)
ZAL	25	[n e] = - [E N]	

A.4. Update the current SASC files

Current SASC files were generated from the slowness and azimuth residuals without the global slowness and azimuth station calibrations (GSASC) proposed in this memo. To avoid duplicate corrections, SASC files for 3C stations must be re-trained to incorporate the GSASC implementation. Besides, there are more training data available since the last SASC files were generated. In this proposal, a set of new SASC files have been generated for primary 3C stations and arrays except ABKT, BRAR, CPUP, KBZ, NOA, PDY, ROSC and ZAL.

A new grid file has been defined to include regional and local seismic-phase slownesses. The maximum slowness boundary is extended from 15 sec/deg to 40 sec/deg. This new grid will result in applying the SASC bin corrections to all possible observed detections in the automatic system.

Training data were selected using the same criteria used in the previous SASC proposal (Bondar, 1998). The selected events have to be located by at least five stations with azimuthal gap less than 180 degrees. The arrivals belonging to the selected events have to be time-defining phases with high signal-to-noise ratio (whose attribute ***detection****.fstat* > 10 at arrays and ***arrival.****rect* > 0.9 at 3-component stations). All detections were selected from the REB between January 1, 1995 and March 31, 1998.

For selected training arrivals at 3C stations, the slowness and azimuth were firstly corrected by the GSASC. The modified slowness and azimuth residuals were then used to generate new SASC files.

Figure 3 is an example of new SASC for station DBIC. The vectors point from the center of the bins to the location (marked by a diamond symbol) where the entire bin would be shifted when the specific bin correction is applied. For comparison purpose, Figure 4 shows the current correction vectors. We can see that slowness-azimuth corrections are reduced in the new SASC because of the GSASC implementation. New SASC maps of primary 3C stations and arrays are shown in Figures 23-48. These corrections are recommended following the global ***polar-alpha*** and ***SEMA*** corrections for slowness and azimuth observations. If the sitechan.hang values are not altered in the database, we have prepared SASCs that would correct azimuth with the ***SEMA*** rotation in all slowness bins.

Table 5 lists the comparisons between the current (old) and new SASCs for 3C primary stations, and Table 6 lists the comparisons between the current (old) and new SASCs for primary arrays. In the tables 5 and 6, **Nobs** is the total number of observations, the columns **Ncor** and **%** are the number and percentage of observations contributed to the corrections, respectively. The column **Ncb** is the number of bins with SASC corrections. The column **Trend** denote whether there is a global trend for slowness residual vectors, and the last column denotes whether the regional and local slowness correction is applied. In general, the new SASCs have more correction bins. The global trends of the slowness residual vectors at arrays CMAR, PDAR and TXAR are still kept. As the correction grid has been extended to the regional and local slowness range, the new SASC files at three arrays, ASAR, GERES and KSAR, have bin corrections for regional seismic phases.

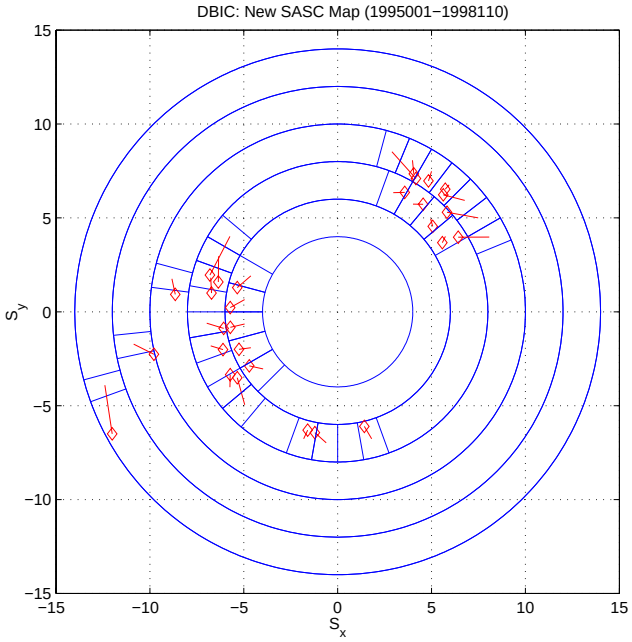

Figure 3. New SASC map for DBIC. After applying the GSASC to observed slowness and azimuth values, slowness-azimuth corrections are reduced compared to the current SASC as shown in Figure 4.

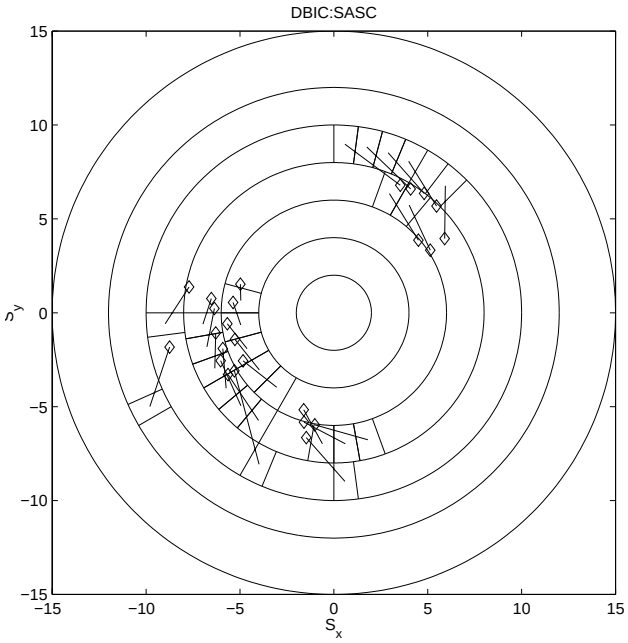

Figure 4. Current SASC map for DBIC. The rotational pattern of azimuth corrections indicates possible incorrect sensor orientation. The in-ward pattern of slowness corrections implies systematic over-estimation of slowness.

Table 5: Comparisons of the old and new SASCs for primary 3C stations

STA	version	Nobs	Ncor	%	Ncb	Trend	Regional correction
BDFB	old	3385	548	16.2	17	not found in all 3C stations	not applied in all 3C stations
	new	4490	901	20.1	27		
BGCA	old	5218	1726	33.1	48		
	new	5635	2787	49.5	50		
BJT	old	1180	260	22.0	9		
	new	1931	372	19.3	16		
BOSA	old	2261	656	29.0	20		
	new	3174	724	22.8	19		
DBIC	old	3275	893	27.3	25		
	new	4766	1433	30.1	29		
HIA	old	466	173	37.1	9		
	new	1221	647	53.0	29		
LPAZ	old	2330	216	9.3	10		
	new	3860	116	3.0	5		
MAW	old	2666	1623	60.9	35		
	new	3565	2008	56.3	25		
MNV	old	830	153	18.4	3		
	new	1509	328	21.7	13		
PLCA	old	3348	772	23.1	18		
	new	4906	938	19.1	16		
SCHQ	old	2310	920	39.8	32		
	new	2862	1313	45.9	33		
STKA	old	6678	4037	60.5	46		
	new	8803	4823	54.8	47		
ULM	old	3432	1995	58.1	39		
	new	4926	2568	52.1	37		
VNDA	old	1942	1327	68.3	25		
	new	3001	1984	66.1	32		

Table 6: Comparisons of the old and new SASCs at primary arrays

STA	version	Nobs	Ncor	%	Ncb	Trend	Regional correction
ARCES	old	7327	5047	68.9	53	N	N
	new	10525	7233	68.7	57	N	N
ASAR	old	12798	10618	83.0	94	N	N
	new	18827	14331	76.1	94	N	Y
CMAR	old	7609	6354	83.5	72	Y	N
	new	11861	9934	83.8	97	Y	N
ESDC	old	3547	2711	76.4	48	N	N
	new	4904	3831	78.1	57	N	N
FINES	old	8703	3736	42.9	29	N	N
	new	12615	5739	45.5	36	N	N
GERES	old	7439	3369	45.3	26	N	N
	new	10463	4981	47.6	43	N	Y
ILAR	old	4385	1815	41.4	36	N	N
	new	8697	4421	50.8	51	N	N
KSAR	old	2733	2363	86.5	56	N	N
	new	4982	4175	83.8	85	N	Y
MJAR	old	1451	1091	75.2	31	N	N
	new	2106	1511	71.7	38	N	N
PDAR	old	6192	1886	30.5	20	Y	N
	new	9420	3869	41.1	31	Y	N
TXAR	old	7146	3487	48.8	32	Y	N
	new	10502	5485	52.2	40	Y	N
WRA	old	6577	5902	89.7	77	N	N
	new	9918	8401	84.7	94	N	N
YKA	old	7115	6123	86.1	58	N	N
	new	10315	8934	86.6	68	N	N

A.5. Testing results

A.5.1 On-line testing for the GSASC

To validate the proposed GSASC, on-line testing with new station-specific values of the slowness parameter, ***polar-alpha***, and inferred sensor orientation was carried out on the testbed for 20 days (1998188-1998207). In the on-line testing, all inferred ***SEMAs*** were used to correct sensor orientations no matter how small the angle is. When testing the GSASC on the testbed, SASCs were turned off at those tested 3C stations for easy analysis. Comparisons have been done among azimuth and slowness residuals by the GSASC in the testbed, the observed residuals, and the corrected residuals by the SASC in operational databases. Figure 5 is an example of the comparison for station DBIC. We can see that the histograms of azimuth and slowness residuals by the GSASC have the smallest bias among the three sets of data. Summary of slowness and azimuth comparisons for all tested stations are listed in Table 7 and Table 8, respectively. In the column 8 of Tables 7, N is total number of phases, and Nc is the number of phases corrected by the SASC. In the column 8 of Tables 8, ***SEMA*** is the orientation correction angle used in the test.

For most stations, expected improvements have been achieved as the median of slowness and azimuth residuals are shifted toward zero. Some of them are even better than the results of SASCs. This is because the SASC only was applied to some detections while GSASC was applied to all detections. However, GSASC get worse performance for slowness estimation at stations BDFB, HIA, and LPAZ. For azimuth, most stations have simple linear relations between medians of residuals of raw data and the corrected data by the GSASC. Only station SCHQ gives a significant worse performance. This is because the mis-orientation at this station was corrected by station operator during June, 1998 (North, personal communication).

The on-line testing confirmed that the GSASCs were working correctly. However, the number of samples are insufficient to conduct significance tests for improvements in median or standard deviations.

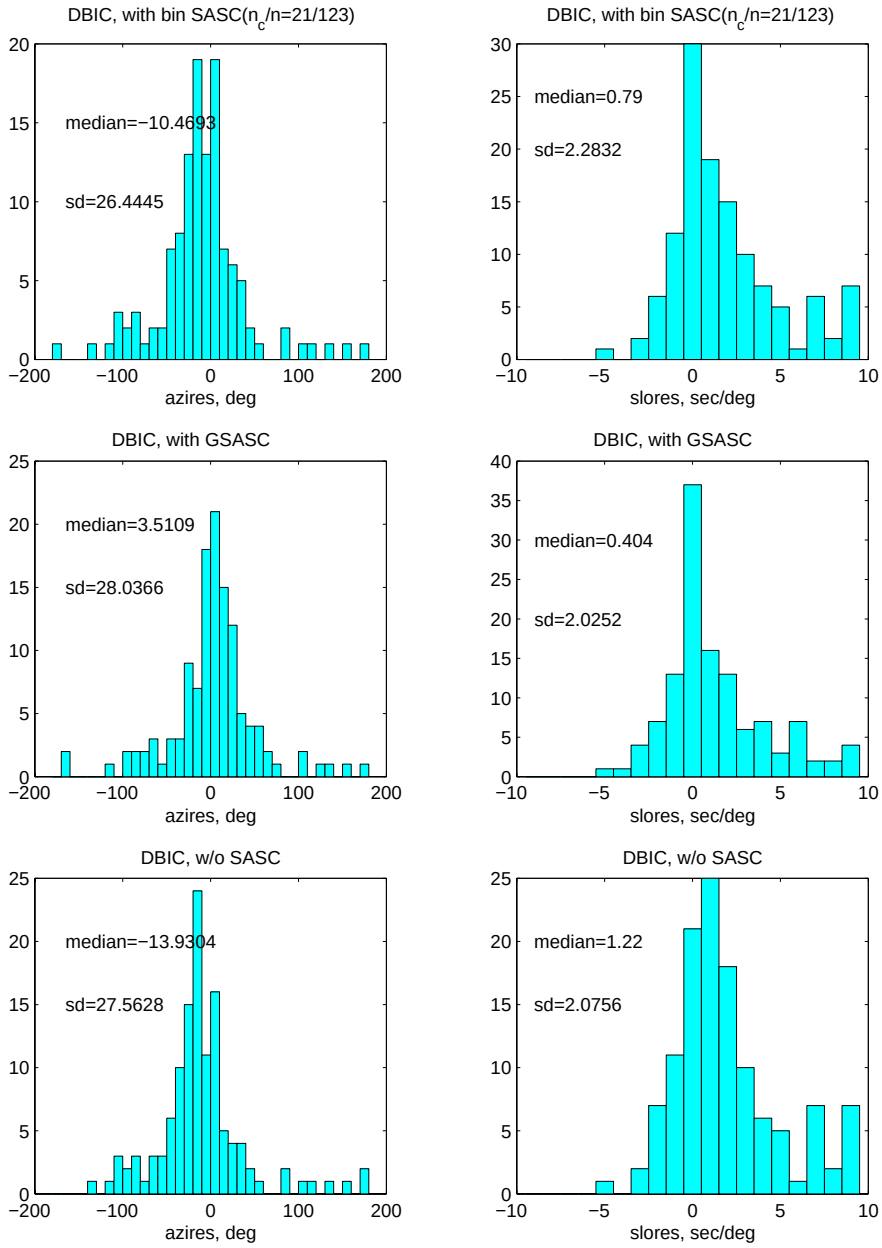

Figure 5. Histograms of slowness and azimuth residuals at DBIC for the uncorrected, GSASC and SASC data, respectively.

Table 7: Comparisons of slowness residuals for on-line testing results

Station	*median*			*Std*			Nc/N
	raw	GSASC	SASC	raw	GSASC	SASC	
BDFB	0.02	1.03	0.2	2.27	2.56	2.03	18/116
BGCA	0.77	0.29	0.46	1.49	1.19	1.26	92/276
BOSA	1.03	0.57	1.03	2.59	2.11	2.49	9/83
CPUP	0.94	0.46	0.94	2.18	2.15	2.18	0/149
DBIC	1.22	0.40	0.79	2.08	2.03	2.28	21/123
HIA	0.48	1.34	0.49	3.08	3.21	2.89	19/119
LPAZ	0.36	1.54	0.41	2.17	2.52	2.13	11/230
MAW	1.56	0.27	0.33	1.64	1.39	1.42	64/121
MNV	-1.19	0.71	-0.52	2.11	2.65	1.89	17/102
PLCA	1.35	0.72	0.86	3.14	2.79	3.09	21/133
SCHQ	1.89	0.66	1.09	2.61	2.07	2.40	14/54
STKA	0.32	0.37	0.24	2.18	2.21	1.65	177/345
ULM	0.04	-0.22	0.13	2.00	1.95	1.88	46/101
VNDA	0.00	-0.33	-0.49	2.45	1.96	1.73	4/9

Table 8: Comparisons of azimuth residuals for on-line testing results

Station	*median*			*Std*			*SEMA*
	raw	GSASC	SASC	raw	GSASC	SASC	
BDFB	-2.5	-1.6	-2.6	32.8	33.1	33.1	1
BGCA	-9.5	0.3	-4.5	14.6	14.8	16.4	10
BOSA	7.9	6.9	7.9	23.6	23.4	23.0	-1
CPUP	4.2	43.0	N/A	110.1	31.0	N/A	-2
DBIC	-13.9	3.5	-10.5	27.6	28.0	26.4	19
HIA	-1.2	-3.4	-1.8	25.0	26.2	24.8	-3
LPAZ	8.5	6.5	8.5	31.7	31.7	31.7	-2
MAW	-6.0	-2.1	-3.5	17.9	16.5	18.1	4
MNV	6.8	-4.5	9.0	25.7	26.7	28.2	-12
PLCA	-5.3	-2.4	-2.6	33.0	31.9	32.1	5
SCHQ	-4.6	16.8	-0.8	22.9	23.0	20.5	21
STKA	3.6	-2.5	0.1	19.4	19.4	15.9	-6
ULM	0.8	1.8	1.5	14.2	14.2	11.3	1
VNDA	-30.8	-22.8	-13.4	19.3	19.3	31.5	8

A.5.2 Off-line testing for the incorporation of GSSC and the modified SASC

This test only implemented the Global Slowness Station Calibration and the related SASC files. Four hours of data (5/11/1998 09:00:00-13:00:00) were off-line tested for phase association and event formation by StaPro and GA. For events that would have associated many defining phases, slowness and azimuth of 3C stations would not be used for location. That is to say, locations of these events would not be changed significantly only because of GSSC implementations at some 3C stations. Here we only compare slowness and azimuth residuals. Table 9 lists the locations of two largest events in the REB and comparisons in the two automatic databases. We can see that the parameters of events are almost identical for the different database. Tables 10 and 11 compare slowness and azimuth residuals in databases REB, SEL3, and GSSC/SASC at the test 3C stations for the two events, respectively. For those phases associated in all three operations, comparisons in the tables show that slowness residuals of some stations were changed while azimuth residuals of all stations are not changed. For those phases associated in the REB but not associated in the automatic databases, usually their slowness and azimuth residuals are very large, no comparison is available. In summary, the GSSC and the related SASC modifications work together properly as expected.

Table 9: Comparisons of locations for different operational databases

date	time	Lat.	Long.	depth	Mb	Region	Database
1998/05/11	10:13:44.2	27.07N	71.76E	0	5.00	India-Pakistan Border	REB
1998/05/11	10:13:52.8	27.13N	71.70E	63.4	4.73		SEL3
1998/05/11	10:13:44.2	27.06N	71.70E	0	5.04		GSSC/ SASC
1998/05/11	12:40:38.4	5.08S	152.50E	10.7	4.90	New Britain Region	REB
1998/05/11	12:40:36.6	5.05S	152.55E	0.36	5.03		SEL3
1998/05/11	12:40:36.5	5.00S	152.63E	0	5.04		GSSC/ SASC

Table 10: Comparisons of slowness and azimuth residuals for Event 1 (1998/05/11 10:13:44.2 27.07N 71.76E India-Pakistan Border Region)

Station	*slores, sec/deg*			*azres, deg*			ARID
	REB	SEL3	GSSC/ SASC	REB	SEL3	GSSC/ SASC	
BGCA	0.74	0.76	0.72	0.7	0.8	0.7	18815399
BJT	-3.29	-3.26	-0.90	1.9	1.8	1.9	18815302
BOSA	-0.28	-0.26	-0.26	-6.1	-6.0	6.0	18815540
DBIC	1.50	1.51	1.55	-16.9	-16.9	-16.9	18815423
HIA	7.66	not associated		-100.9	not associated		18815289
LPAZ	7.04	7.04	9.31	24.5	24.6	24.5	18815547
MAW	7.11	not associated		20.0	not associated		18818726
MNV	2.44	not associated		-25.2	not associated		18815425
SCHQ	11.92	not associated		9.6	not associated		18815277
STKA	-0.65	-0.64	-0.61	23.4	23.4	23.5	18815308
VNDA	7.41	not associated		156.4	not associated		18815644

Table 11: Comparisons of slowness and azimuth residuals for Event 2 (1998/05/11 12:40:38.4 5.08S 152.50E New Britain Region, P.N.G.)

Station	*slores*			*azres*			ARID
	REB	SEL3	GSSC/ SASC	REB	SEL3	GSSC/ SASC	
BDFB	-0.52	-0.53	-0.36	39.7	39.5	39.4	18816629
BGCA	1.99	not associated		-50.1	not associated		18828494
		0.97	0.72		-7.0	-7.0	18816615
BJT	-2.17	-2.17	0.18	-32.5	-32.5	-32.3	18816273
BOSA	6.33	not associated		-28.8	not associated		18816648
DBIC	0.26	not associated		-8.8	not associated		18816639
HIA	0.40	0.40	0.40	-0.9	-0.9	-0.7	18816424
LPAZ	0.69	not associated		8.7	not associated		18816653
MAW	0.86	0.86	0.80	1.8	1.8	1.7	18816434
MNV	-2.11	-2.12	-0.92	15.6	15.6	15.6	18816480
SCHQ	7.71	not associated		29.4	not associated		18828495
STKA	-0.94	-0.94	-0.94	-8.3	-8.3	-8.5	18816287
ULM	1.08	not associated		117.3	not associated		18816415
VNDA	0.01	0.01	0.02	-13.4	-13.5	-13.6	18816546

A.6. Effect of inhomogeneous structures on slowness and azimuth estimation

The GSASC proposed here is under the assumption of that the geological structure beneath the stations is isotropic and lateral homogeneous. Complicated geological structures will result in the complicated pattern of slowness and azimuth residuals. For example, the GSASC did not improve the performance of slowness estimation at station LPAZ during the 20 testing days (see section A5.1). It might be because of very complicated structures around the station. In fact, LPAZ is located in the Bolivian Altiplano at an elevation of 4774 meters, very near the high peaks of the Cordillera Real with elevation of 6446 meters. This situation, together with the proximity to the Pacific Chilean trenches, suggests not only a very thick crust (64 km), which is related to the roots of the mountains, but also some sloping of the Moho discontinuity (Fernandez and Careaga, 1968). Figure 6 shows the individual slowness-azimuth residual vectors for LPAZ. The majority of residual vectors are toward the south-western direction. Namely, the observed slowness values are not systematically greater or smaller than the predicted values, so that the GSASC would not work well.

For a dip Moho structure beneath the station, the observed slowness and azimuth will be distorted. Based on previous studies on this subject (Niazi, 1966; Havskov and Kanasewich, 1978), we can generate a slowness-azimuth residual pattern by assuming a dipping angle and strike direction. Figure 7 is the pattern which ‘best’ matched with the observed slowness-azimuth residuals of LPAZ. Although the pattern is similar to some of the observed residuals, however, it shows that a simple dipping Moho model can not explain the majority anomalous observations. Introduction of a dipping Moho model does not significantly reduce the variance and the model is not recommended.

From the Figure 7 we can see that the slowness and azimuth residuals vary with the slowness and azimuth of incoming seismic waves. In other words, global trends of the slowness-azimuth residual vectors determined in the SASC maps, such as in arrays CMAR, PDAR and TXAR, are not due to a simple dipping Moho, but by more complicated local geological features below the stations.

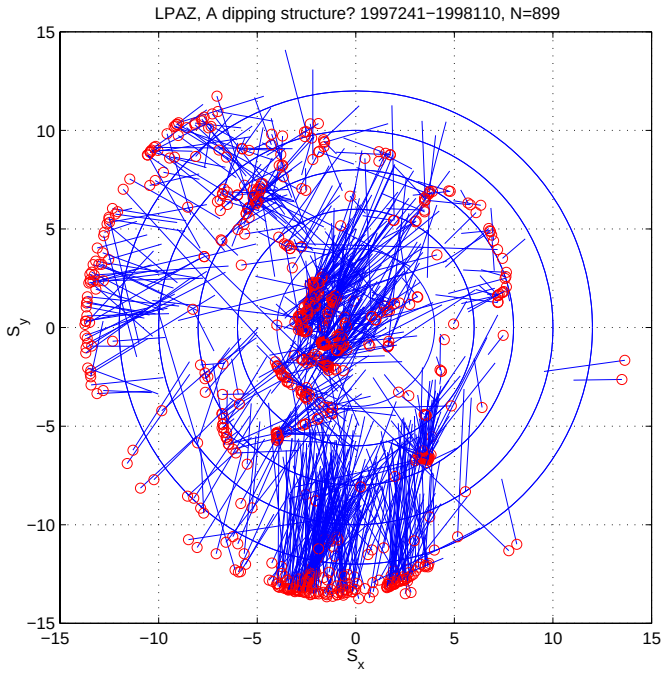

Figure 6. Slowness-azimuth residual vectors for LPAZ. Circles are the predicated slowness and azimuth position while the other end of the vector is the observed position.

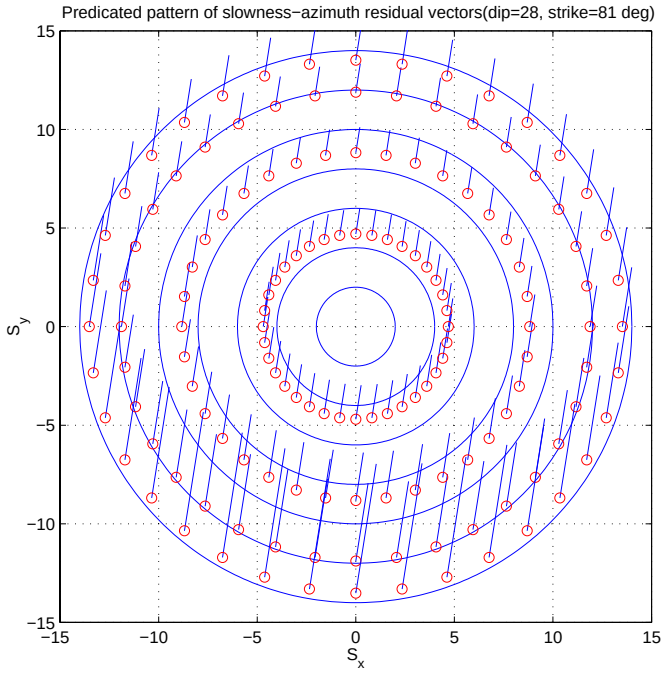

Figure 7. Predicated slowness-azimuth residual vectors for a dipping Moho structures. Circles are the theoretical slowness and azimuth position while the other end of the vector is the predicated observation. The model is not recommended.

A.7. Recommendation to modify the existing DetSASC software

In the current version of the program *DetSASC*, SASC bin correction are determined by the slowness and azimuth residuals in the ***REB***.*assoc* table. After implementation of SASC, however, the slowness and azimuth residuals saved in the ***REB***.*assoc* table are the corrected residual values. Namely,

$$slores = slowness_{observed} - slowness_{predicted} - slowness_{correction}$$

$$azres = azimuth_{observed} - azimuth_{predicted} - azimuth_{correction.}$$

This approach prevents further updating SASC files using only *sloers* and *azres* values in the databases.

We recommend modification of the existing software accordingly to overcome this problem.

A.8. Summary

The GSASC discussed here is a very simple yet effective approach to improve slowness and azimuth estimation with clear physical meanings. It is a first-order approximation for 3C stations while the SASCs are fine-tune corrections in the pre-defined slowness-azimuth bins. The GSASC should have a higher priority than the SASC for 3C stations.

References

Bullen, K. E., An introduction to the theory of seismology, pp. 128-130, *Cambridge University press*, London, 1963.

Bondar, Insvan, Teleseismic slowness-azimuth station corrections (SASC) for the IMS network, *CMR-PRO-98/01*, 1997.

Fernandez, L. M. and J. Careaga, The thickness of the crust in central United States and La Paz, Bolivia, from the spectrum of longitudinal seismic waves, *Bull. Seism. Soc. Am.*, **58**, pp. 711-741, 1968.

Havskov, J. and E. R. Kanasewich, Determination of the dip and strike of the Moho from array analysis, *Bull. Seism. Soc. Am.*, **68**, pp. 1415-1419, 1978.

Niazi, M., Corrections to apparent azimuths and travel-time gradients for a dipping Mohorovicic discontinuity, *Bull. Seism. Soc. Am.*, **56**, pp. 491-509, 1966.

Wang, Jin and Richard Stead, Remote checking of channel Status for 3C seismic stations at the PIDC, *Technical Report CMR-98/11*, 1998.

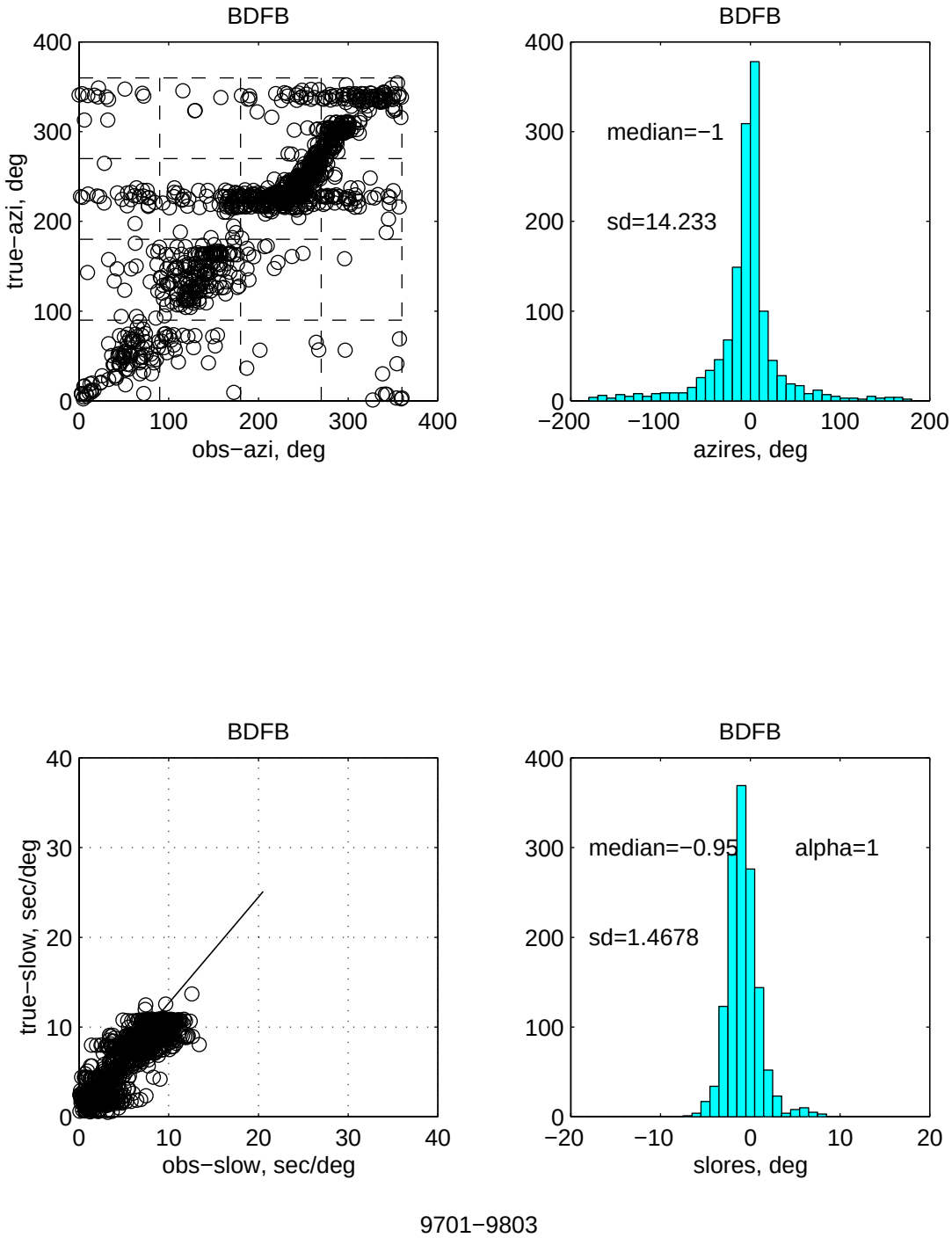

Figure 8. Relations between the observed azimuth/slowness and true azimuth/slowness values, and histograms of azimuth/slowness residuals for station BDFB. It shows the slowness determination at BDFB are under-estimated systematically.

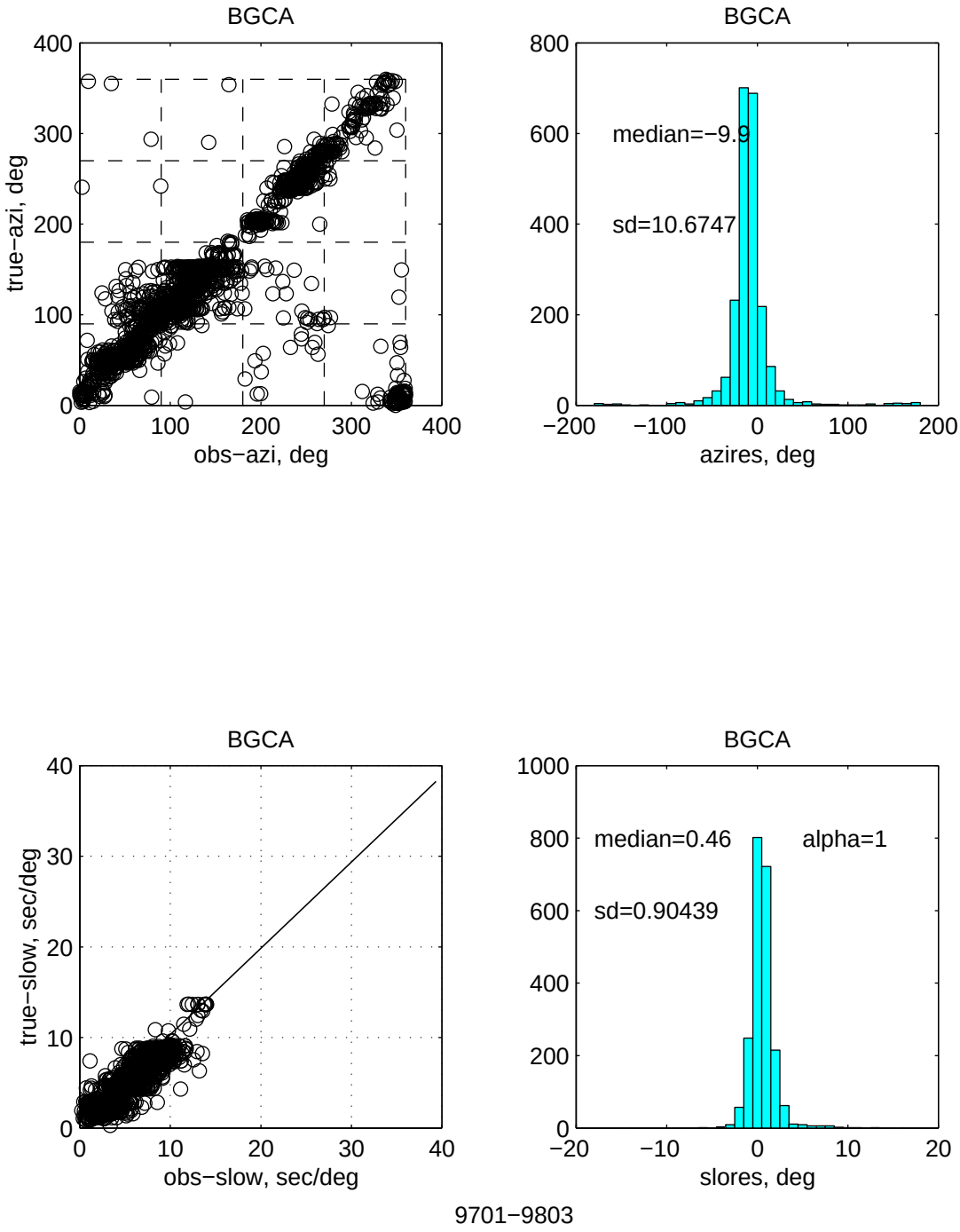

Figure 8. Relations between the observed azimuth/slowness and true azimuth/slowness values, and histograms of azimuth/slowness residuals for station BGCA. It shows the azimuth estimations have 10 degrees bias, and the slowness determination are over-estimated systematically at BGCA.

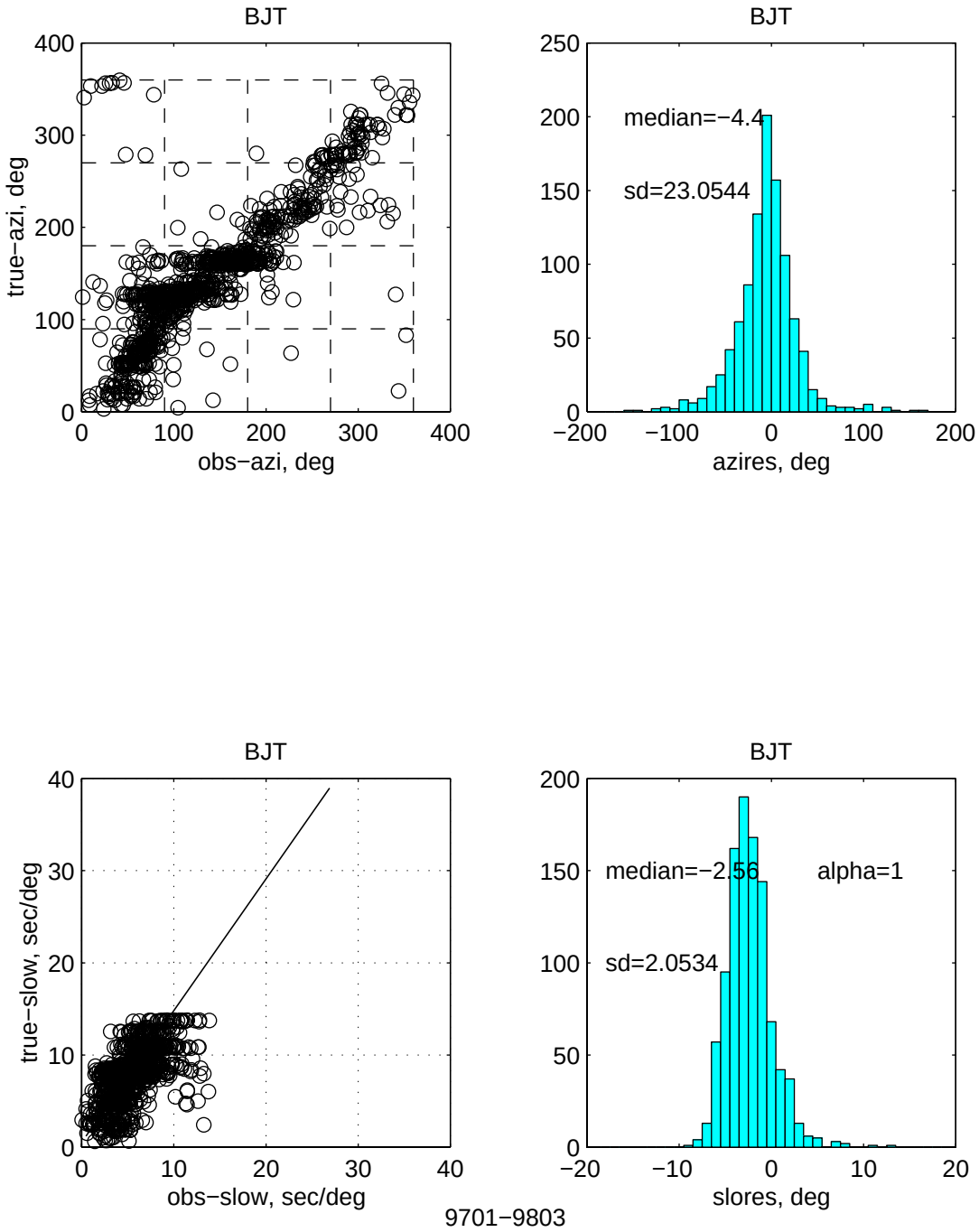

Figure 9. Relations between the observed azimuth/slowness and true azimuth/slowness values, and histograms of azimuth/slowness residuals for station BJT. It shows the slowness determination at BDFB are under-estimated systematically. It shows the slowness determination at BJT are systematically under-estimated.

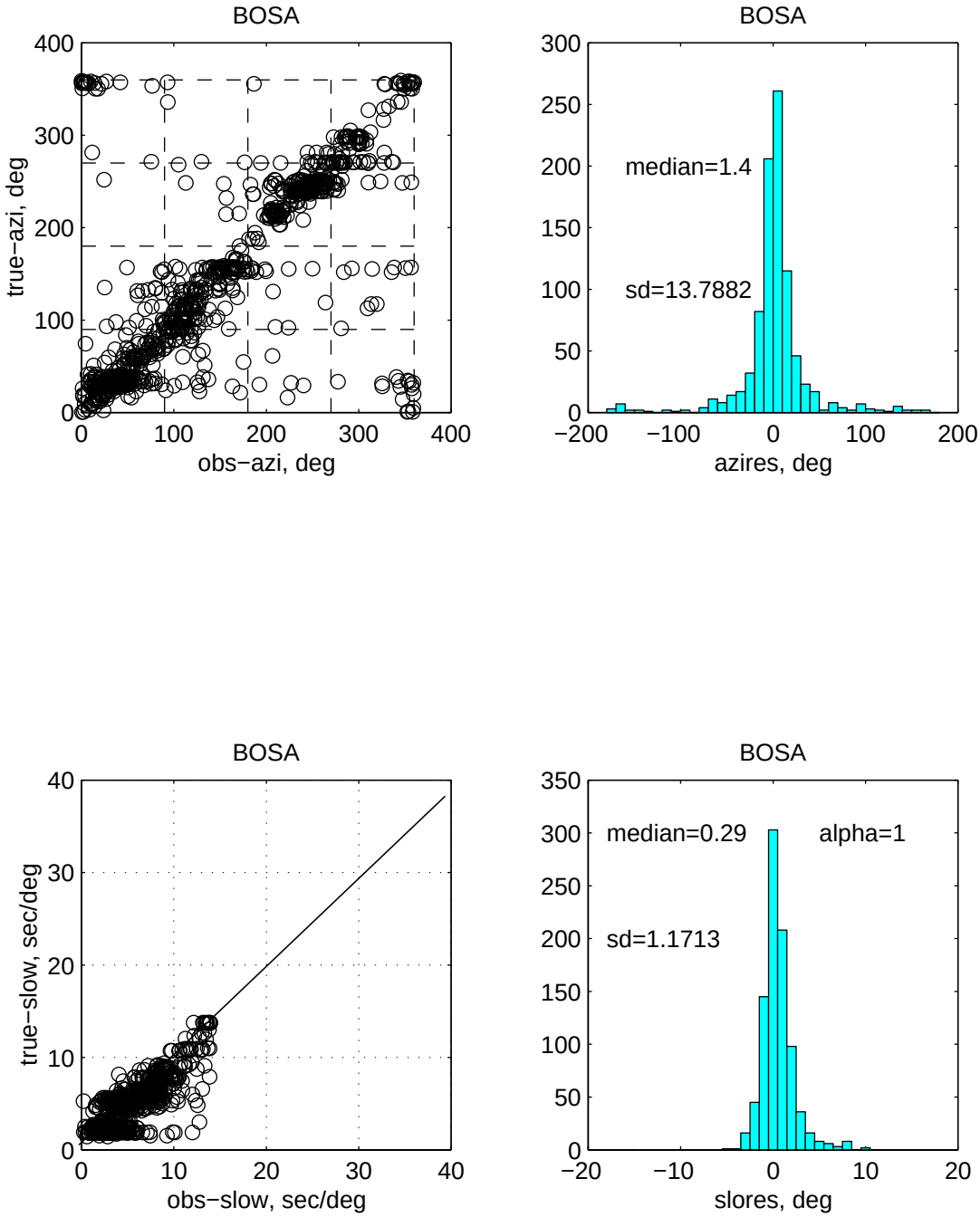

Figure 10. Relations between the observed azimuth/slowness and true azimuth/slowness values, and histograms of azimuth/slowness residuals for station BOSA. It shows the slowness determination at BOSA are over-estimated systematically.

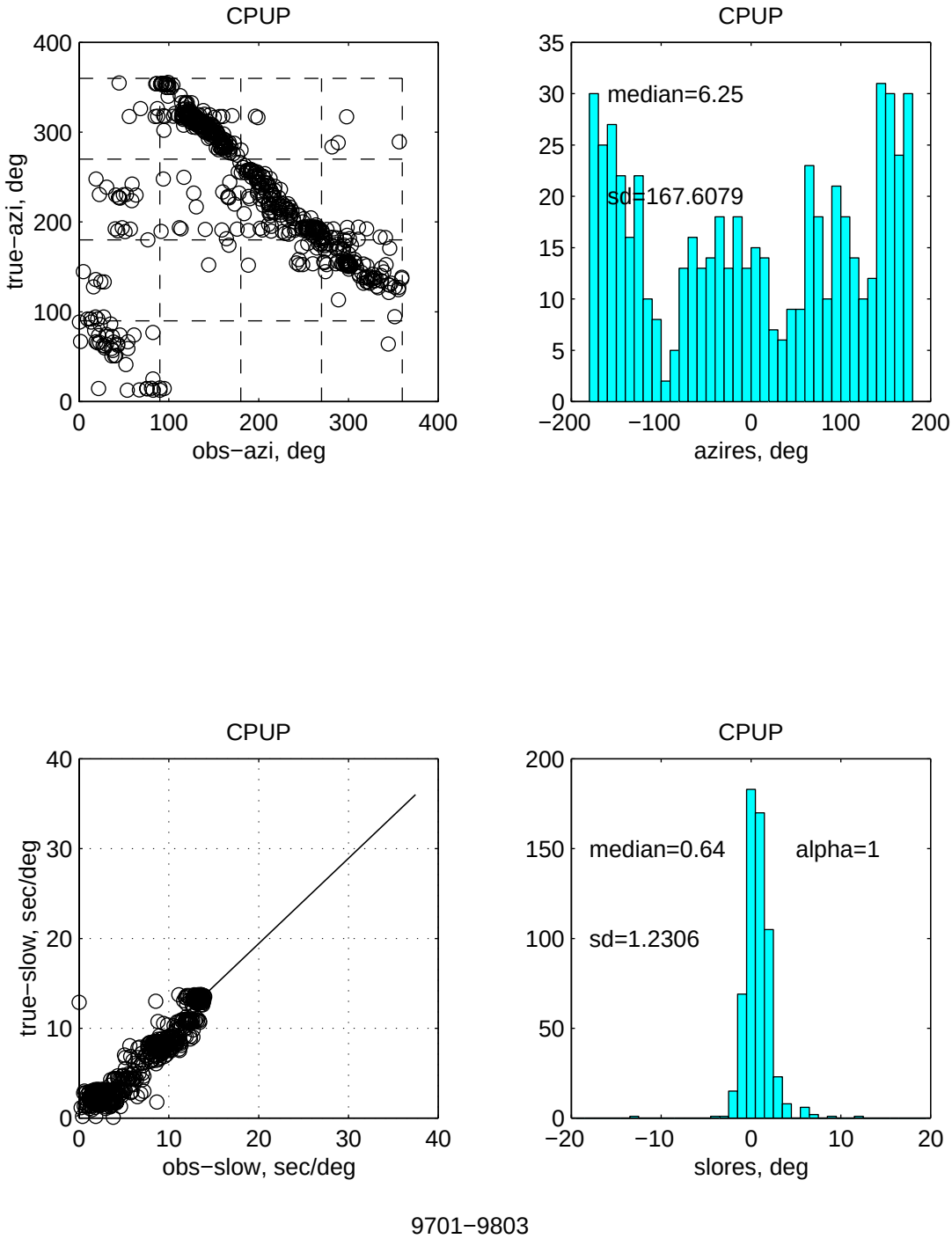

Figure 11. Relations between the observed azimuth/slowness and true azimuth/slowness values, and histograms of azimuth/slowness residuals for station CPUP. It shows the two horizontal channels were treated incorrectly, and the slowness determination at CPUP are over-estimated systematically.

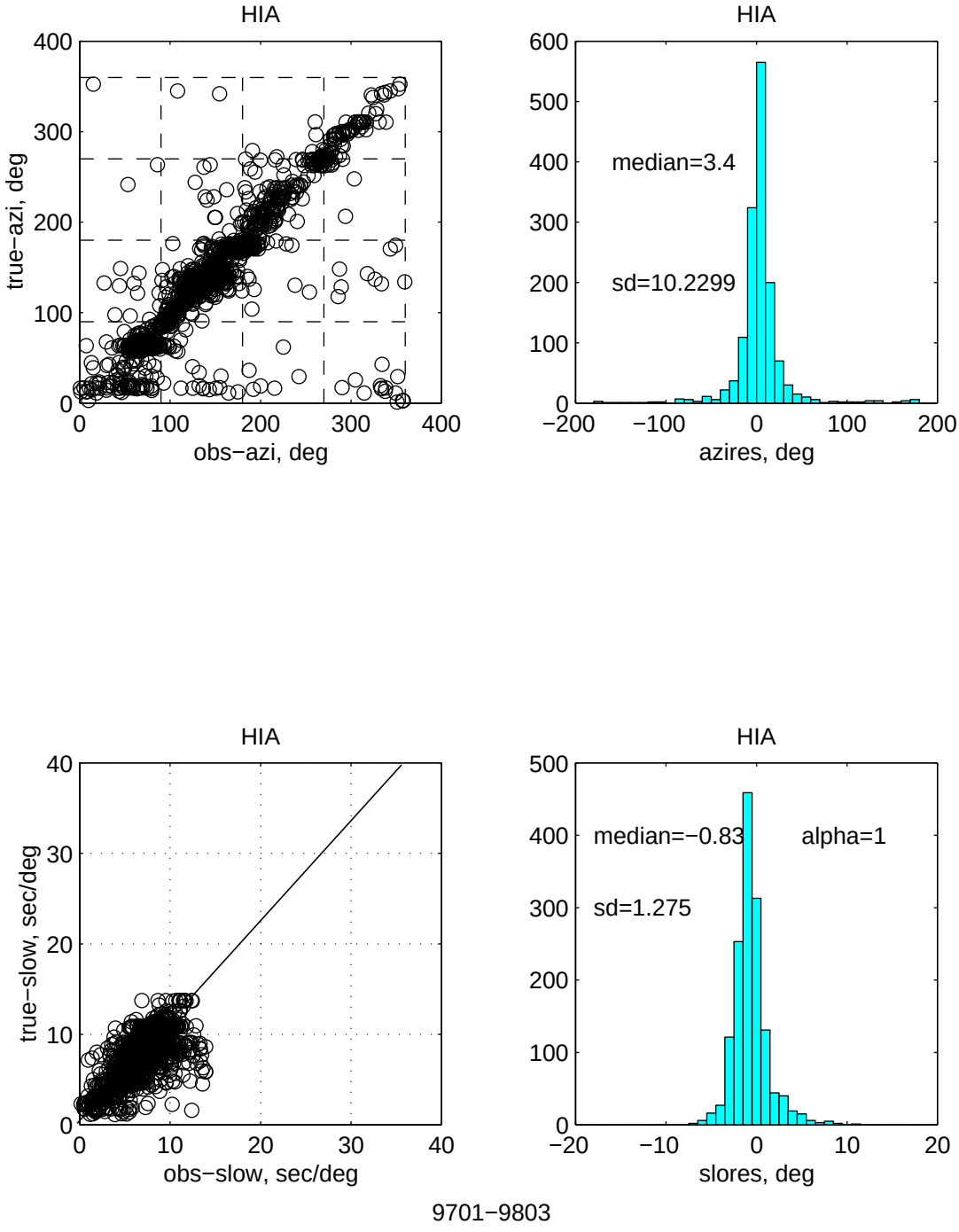

Figure 12. Relations between the observed azimuth/slowness and true azimuth/slowness values, and histograms of azimuth/slowness residuals for station HIA. It shows the slowness determination at HIA are under-estimated systematically.

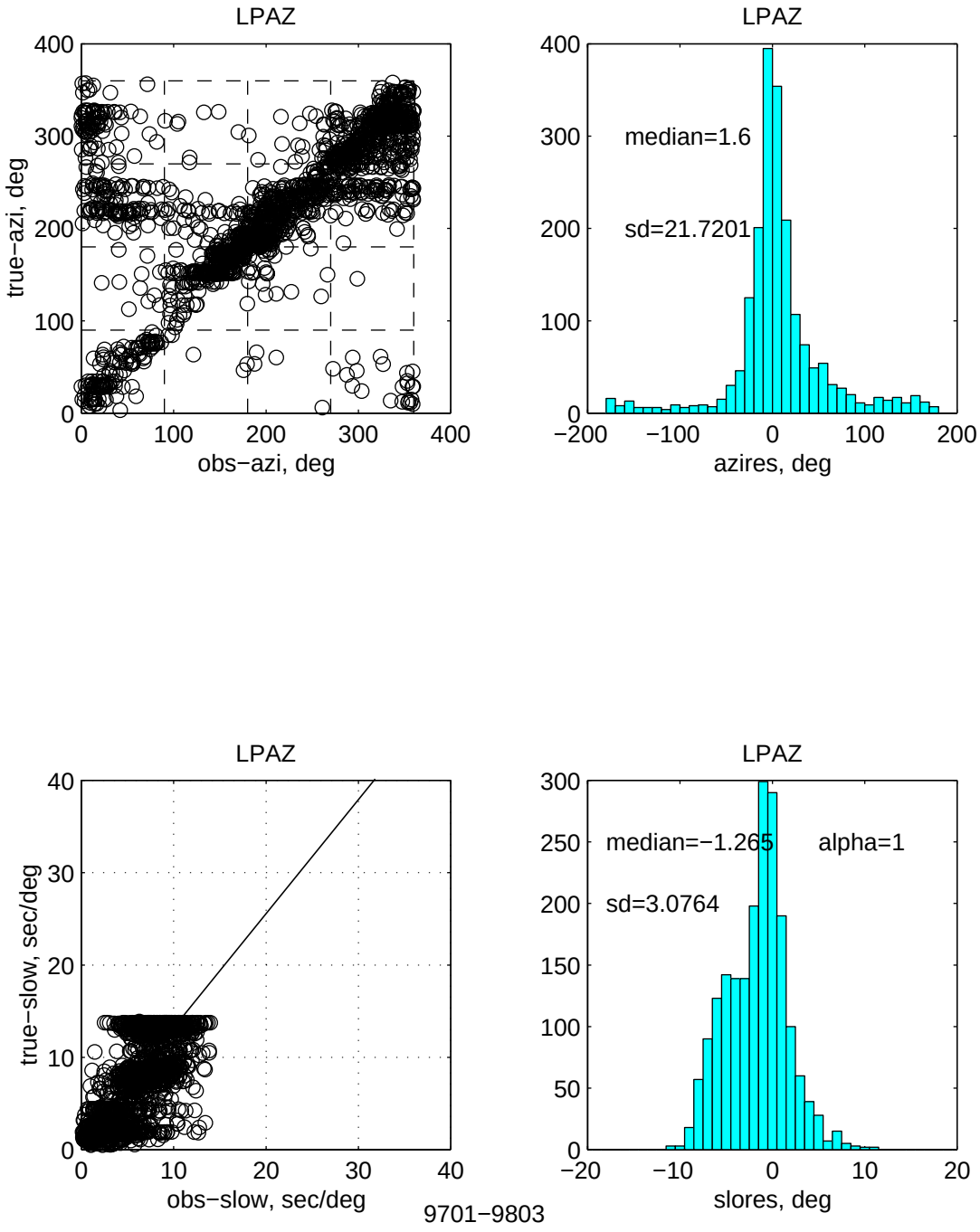

Figure 13. Relations between the observed azimuth/slowness and true azimuth/slowness values, and histograms of azimuth/slowness residuals for station LPAZ. It shows the slowness determination at LPAZ are under-estimated in overall. More analysis (Figures 6 and 7) shows the local geology is very complicated.

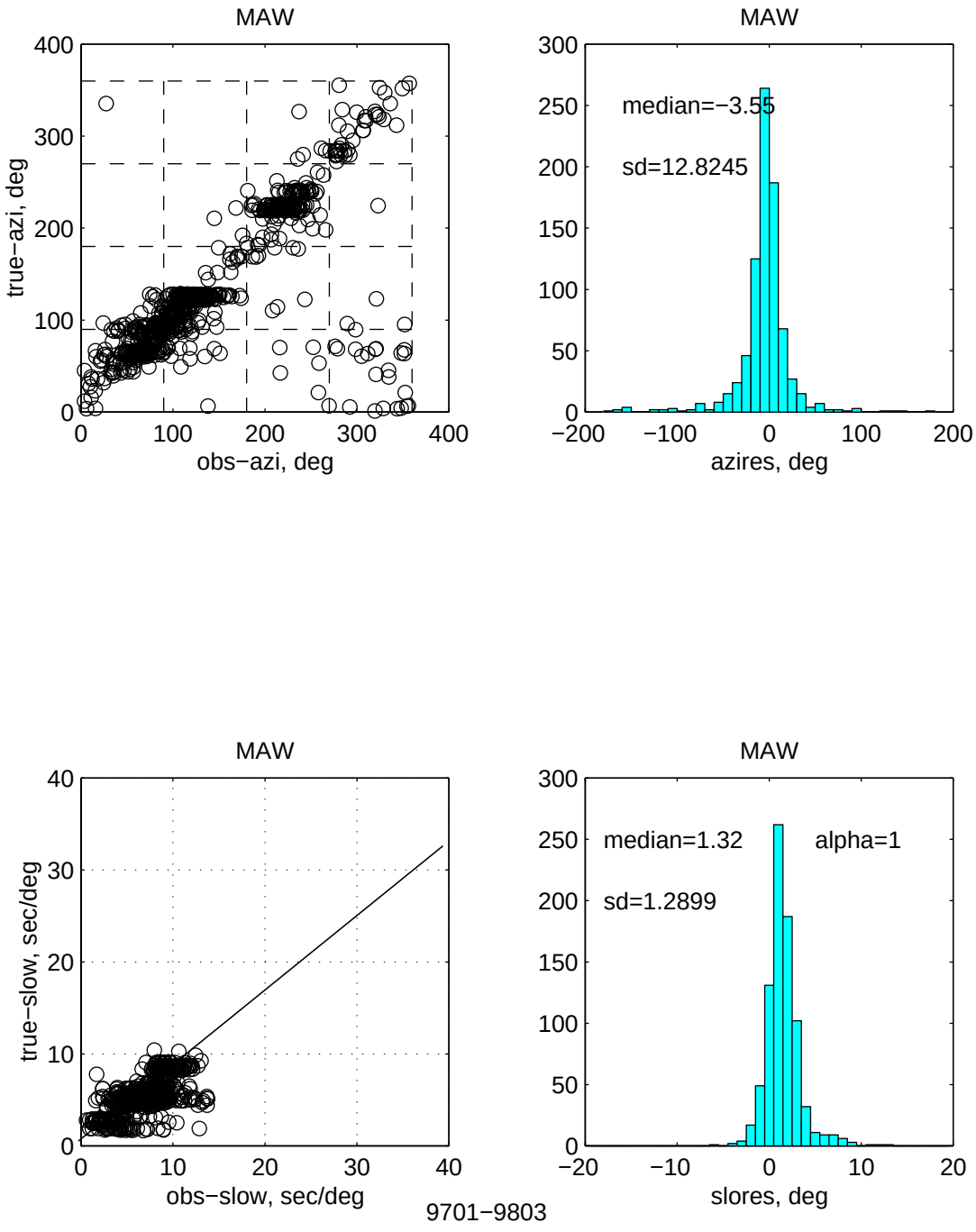

Figure 14. Relations between the observed azimuth/slowness and true azimuth/slowness values, and histograms of azimuth/slowness residuals for station MAW. It shows the slowness determination at MAW are systematically over-estimated.

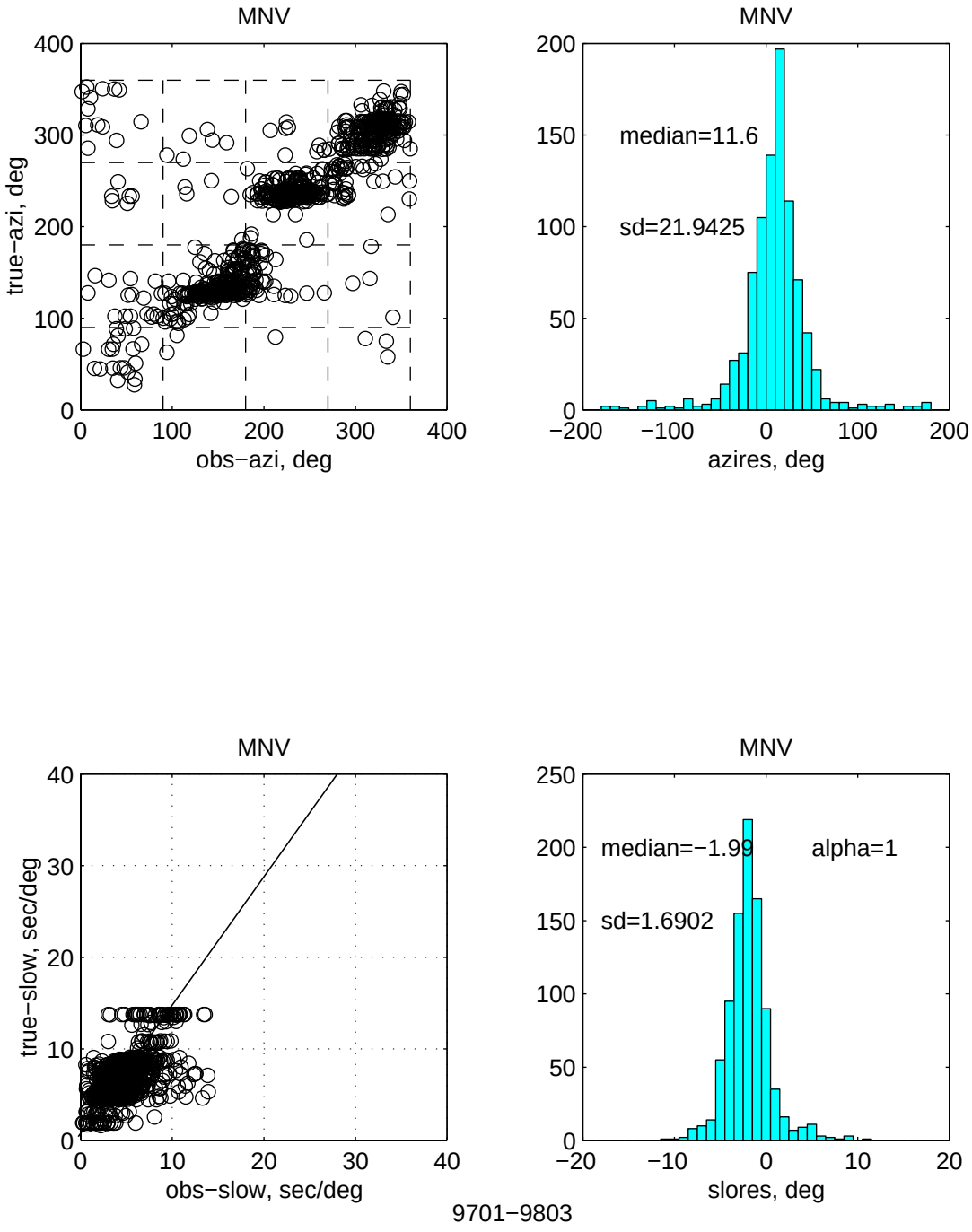

Figure 15. Relations between the observed azimuth/slowness and true azimuth/slowness values, and histograms of azimuth/slowness residuals for station MNV. It shows the azimuth estimations have 12 degrees bias, and the slowness determination at MNV are under-estimated systematically.

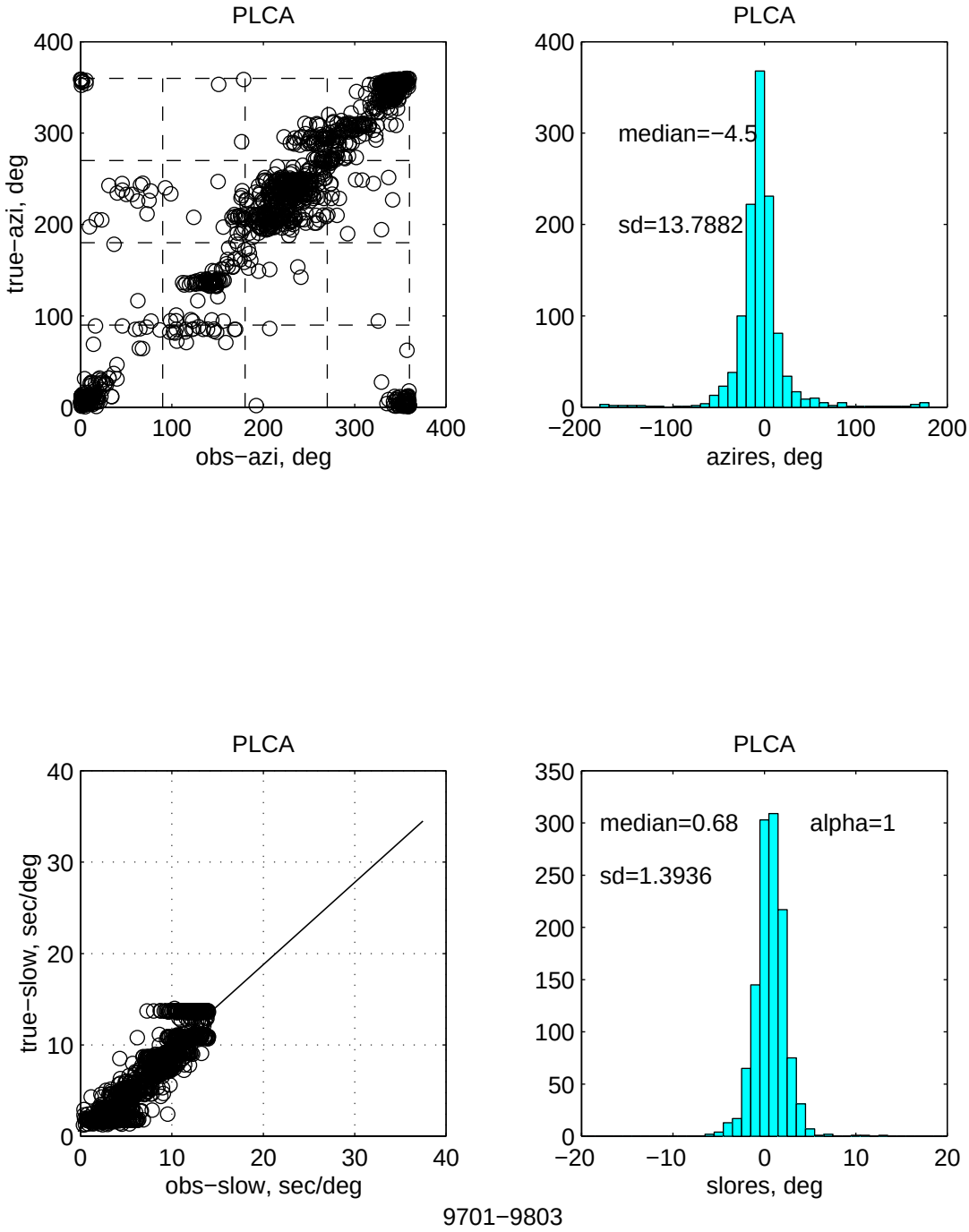

Figure 16. Relations between the observed azimuth/slowness and true azimuth/slowness values, and histograms of azimuth/slowness residuals for station PLCA. It shows the azimuth estimations have 5 degrees bias, and the slowness determination at PLCA are over-estimated systematically.

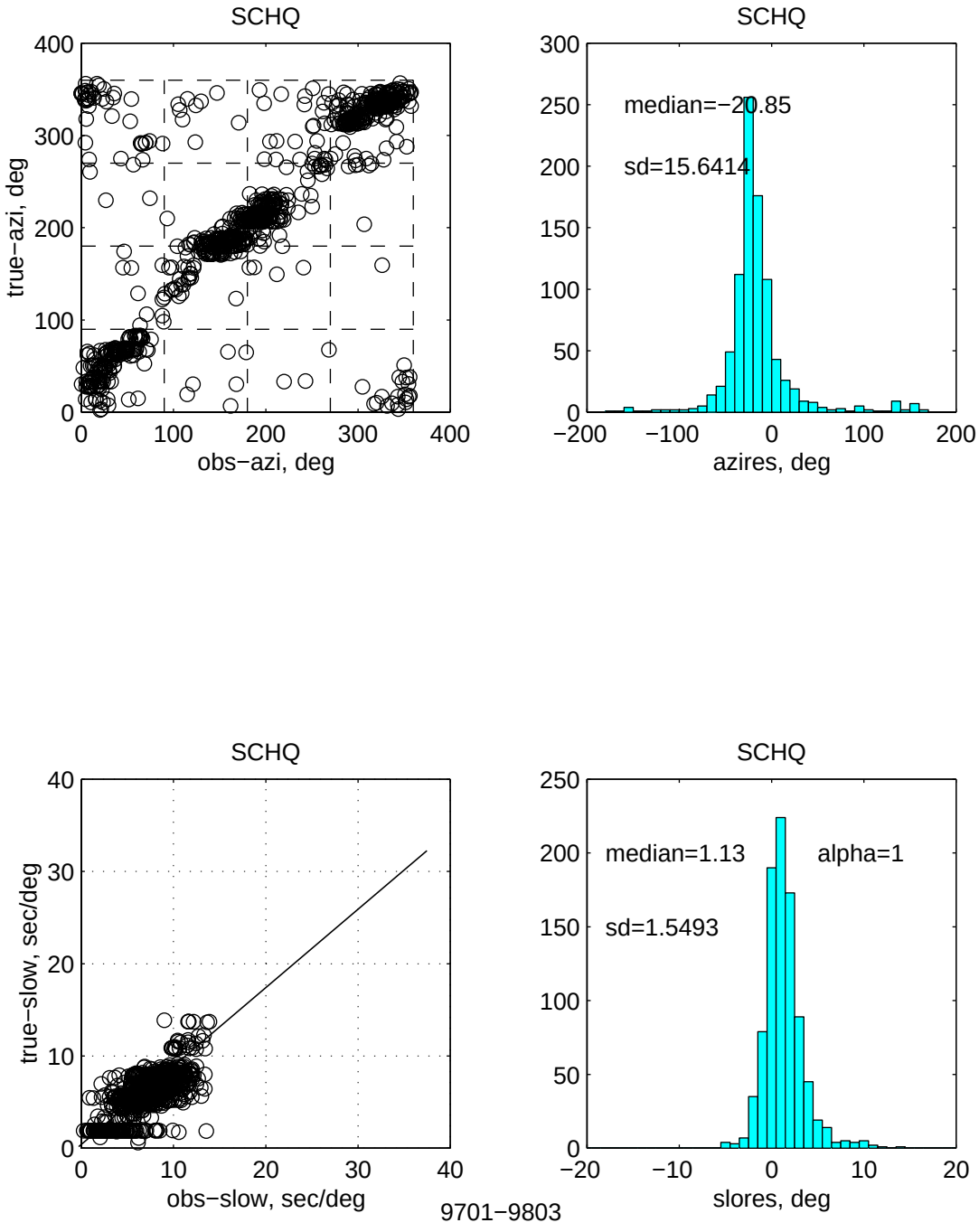

Figure 17. Relations between the observed azimuth/slowness and true azimuth/slowness values, and histograms of azimuth/slowness residuals for station BDFB. It shows the azimuth estimations have 21 degrees bias, and the slowness determination at SCHQ are over-estimated systematically.It shows the slowness determination at BDFB are under-estimated systematically.

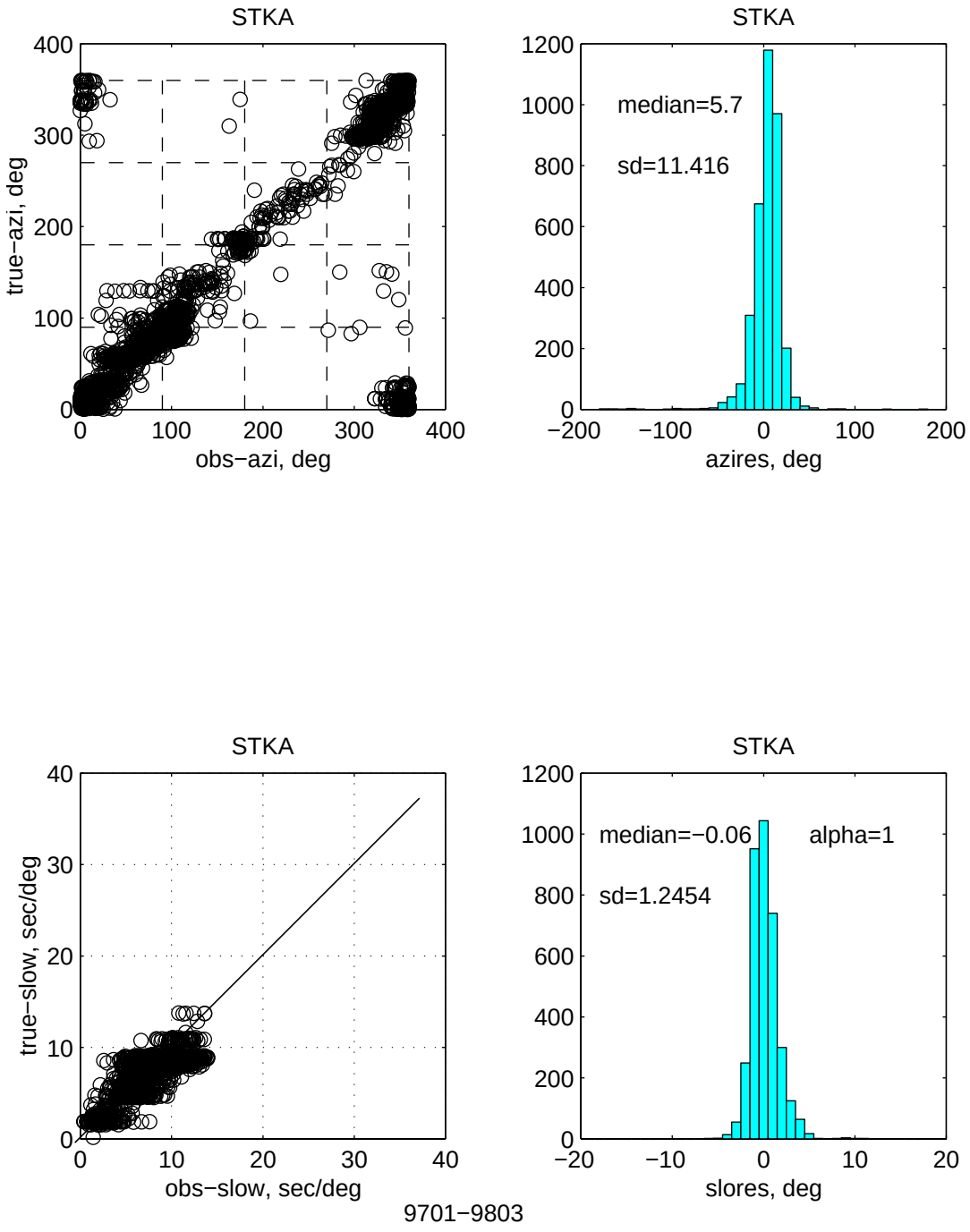

Figure 18. Relations between the observed azimuth/slowness and true azimuth/slowness values, and histograms of azimuth/slowness residuals for station STKA. It shows the azimuth estimations have 6 degrees bias, and the slowness determination at STKA are quite good.

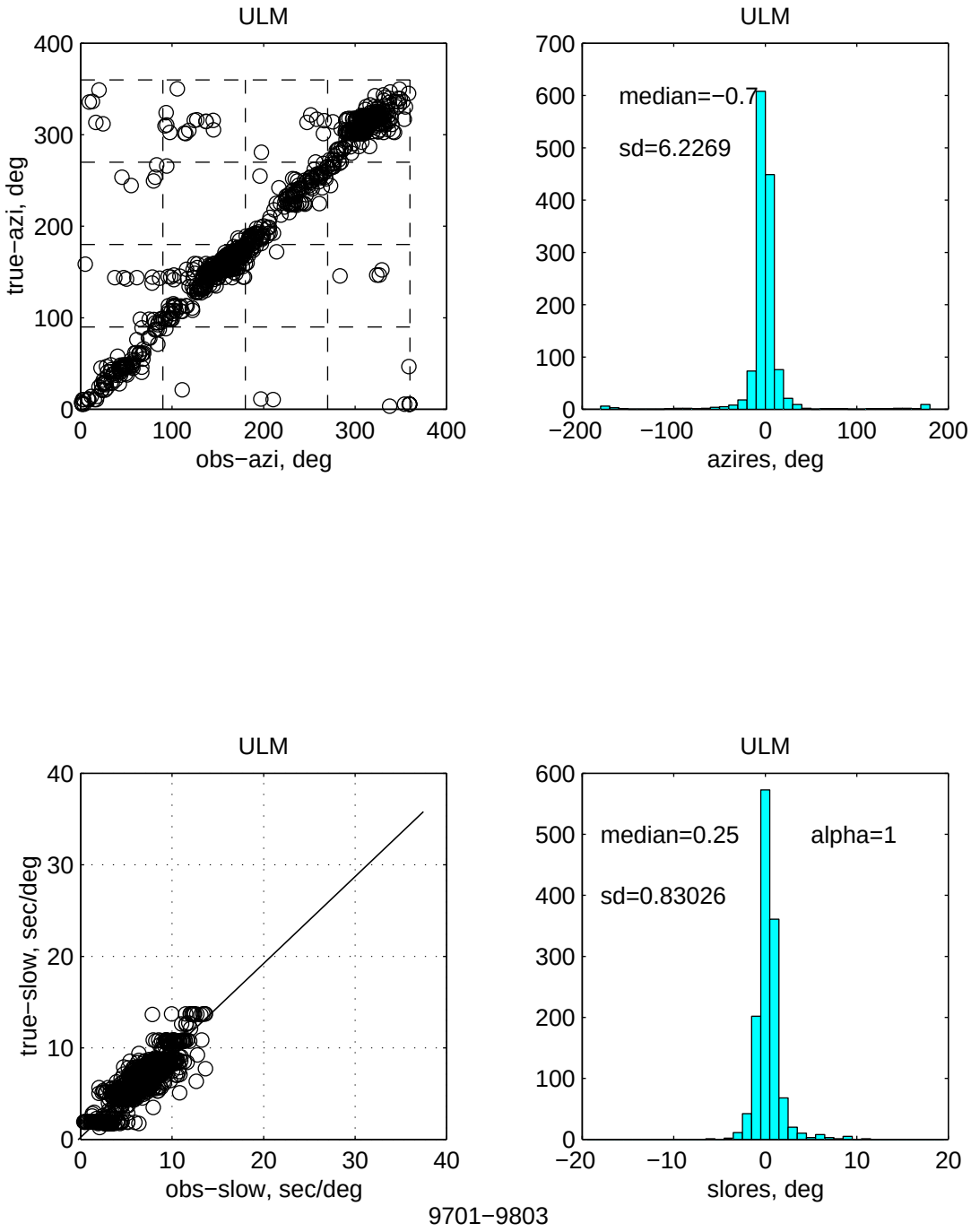

Figure 19. Relations between the observed azimuth/slowness and true azimuth/slowness values, and histograms of azimuth/slowness residuals for station ULM. It shows the slowness determination at ULM are over-estimated systematically.

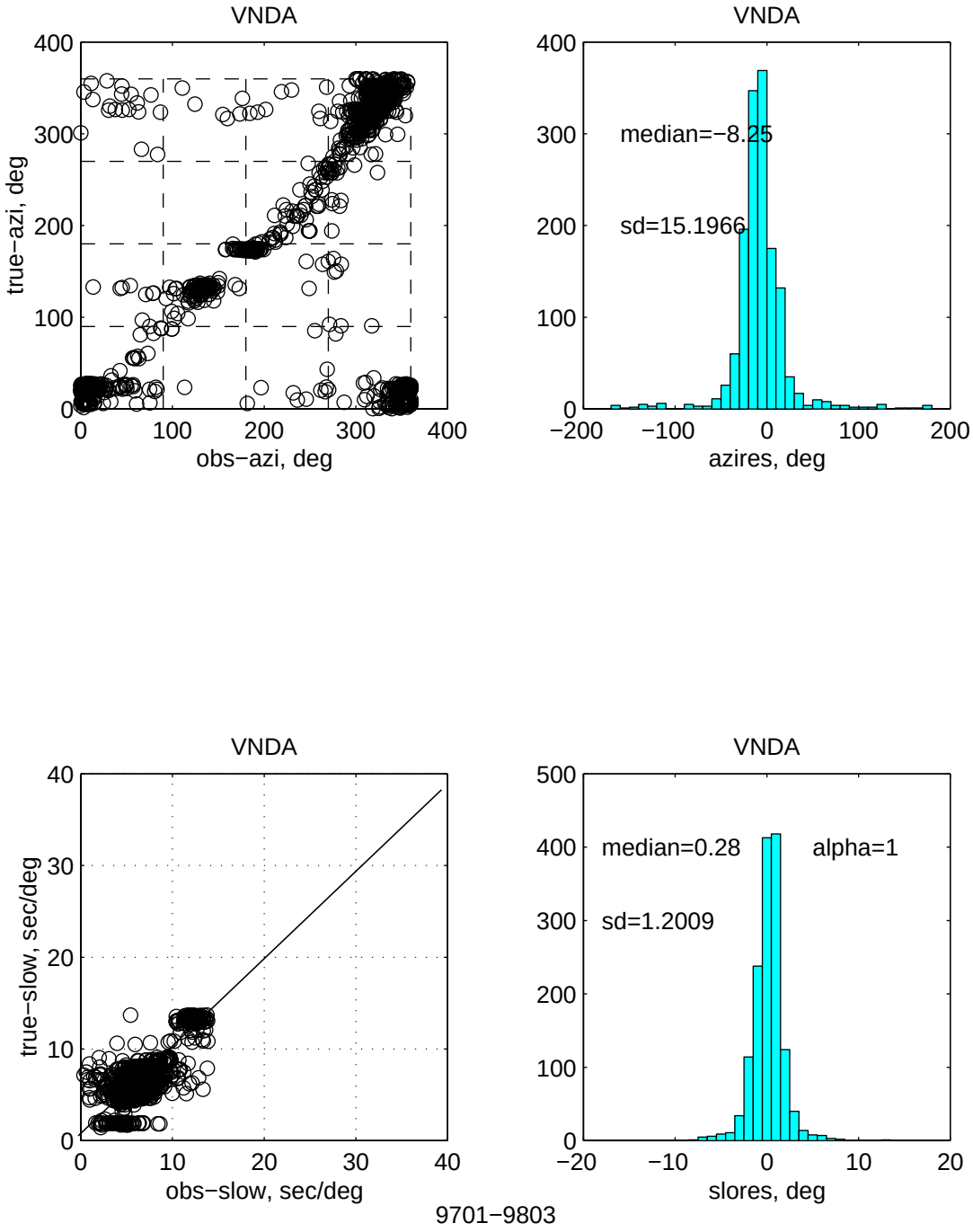

Figure 20. Relations between the observed azimuth/slowness and true azimuth/slowness values, and histograms of azimuth/slowness residuals for station VNDA. It shows the azimuth estimations have 8 degrees bias, and the slowness determination at VNDA are over-estimated systematically.

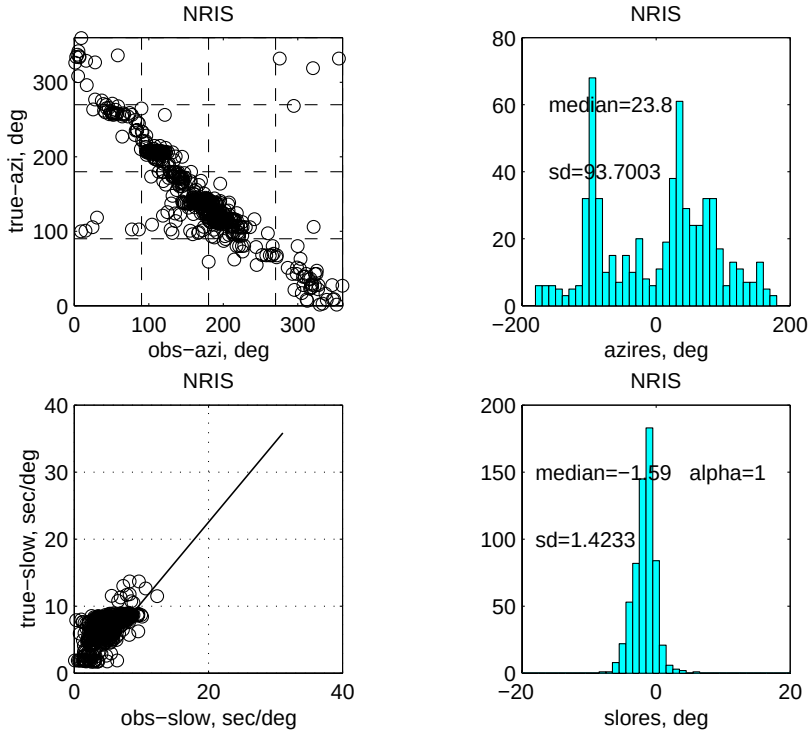

Figure 21. NRIS is a tri-axial station and the special analysis shows the three channels are incorrectly connected. The slowness determination at NRIS are under-estimated systematically.

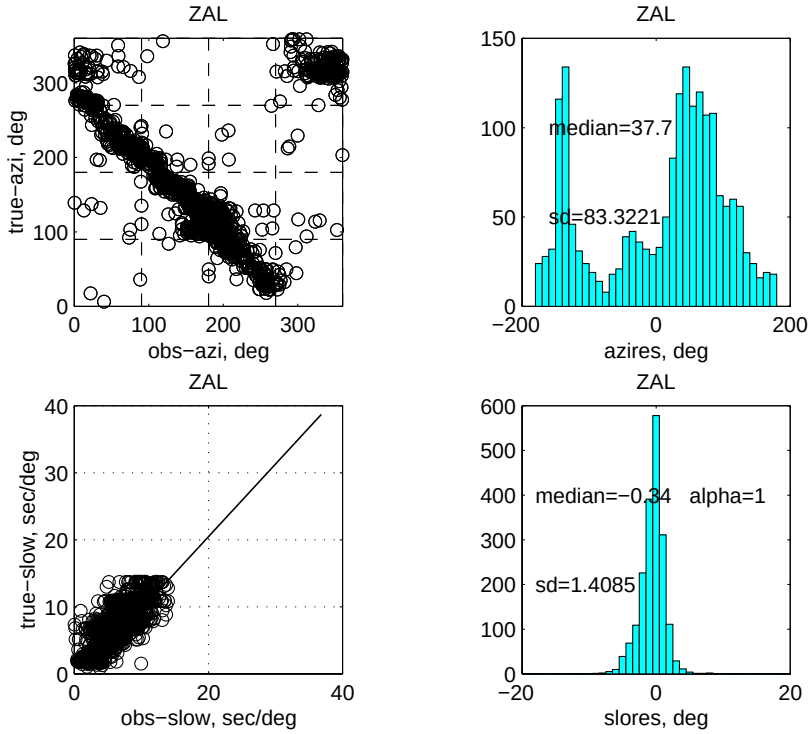

Figure 22. ZAL is a tri-axial station and the special analysis shows the three channels are incorrectly connected.

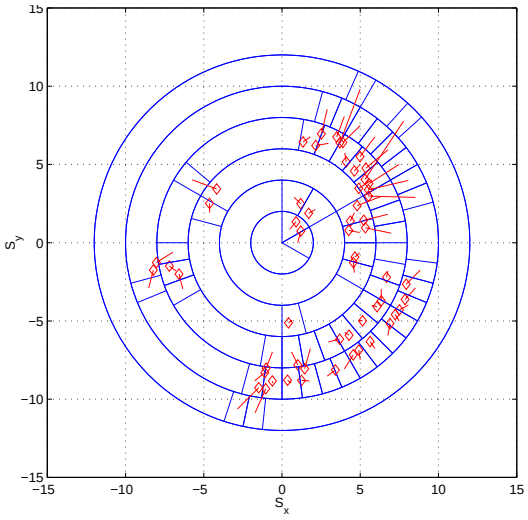

Figure 23. New SASC map for ARCES.

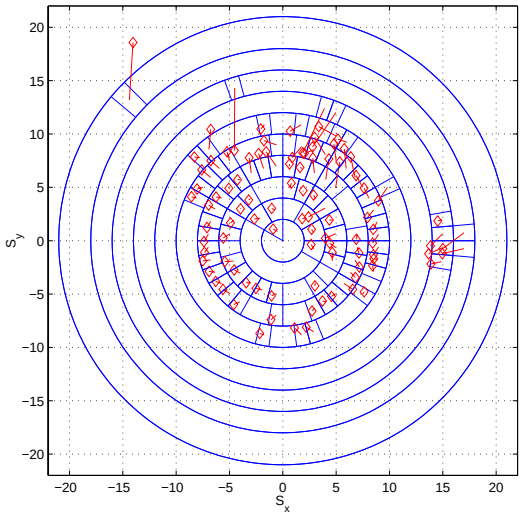

Figure 24. New SASC map for ASAR

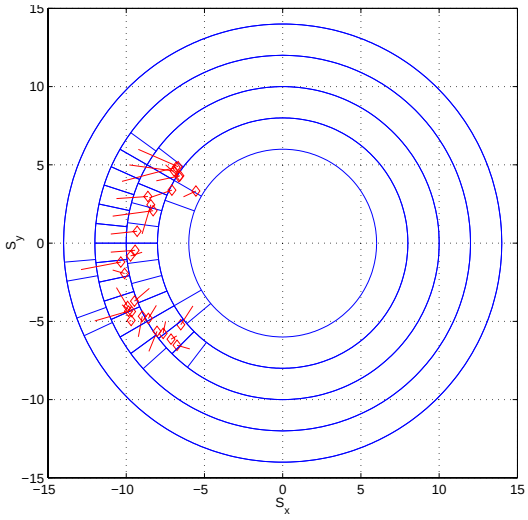

Figure 25. New SASC map for BDFB.

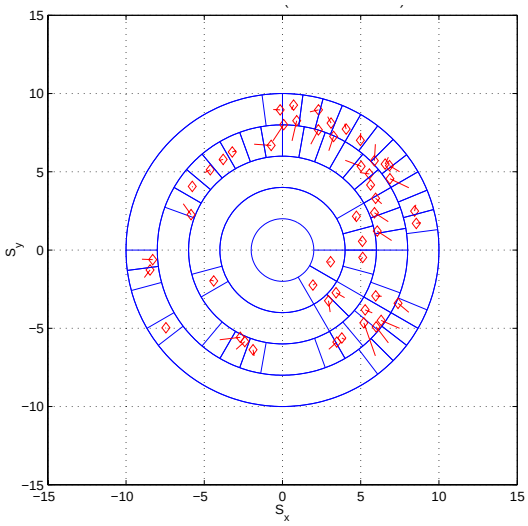

Figure 26. New SASC map for BGCA

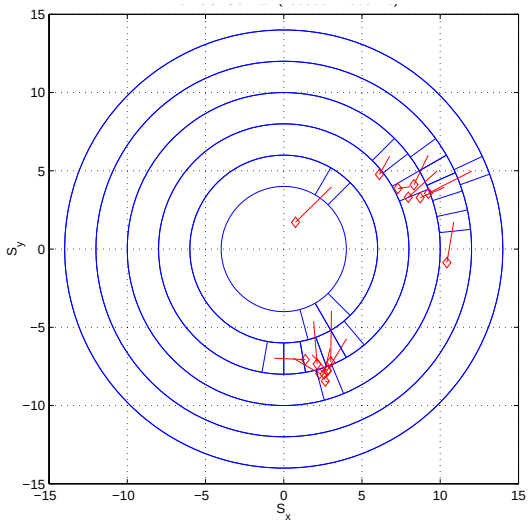

Figure 27. New SASC map for BJT.

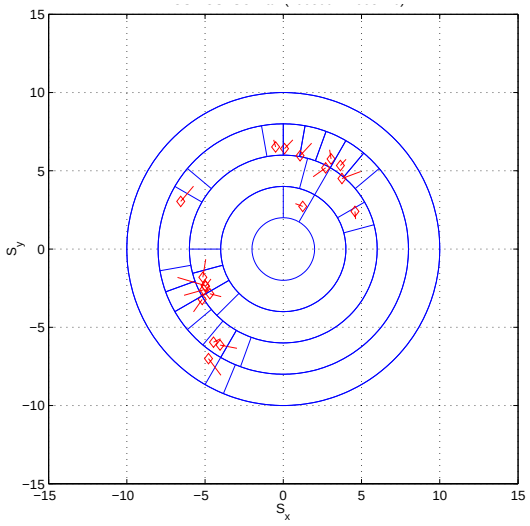

Figure 28. New SASC map for BOSA.

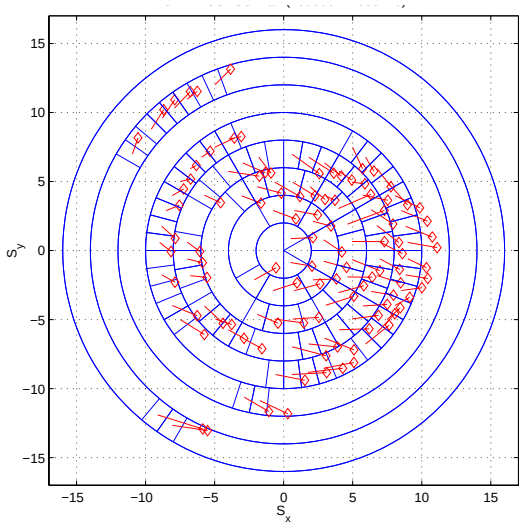

Figure 29. New SASC map for CMAR.

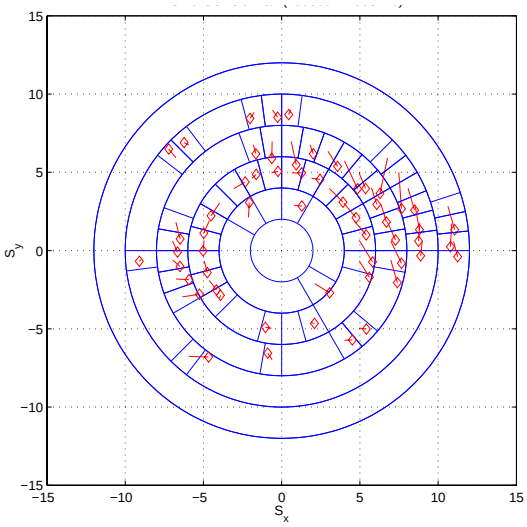

Figure 30. New SASC map for ESDC.

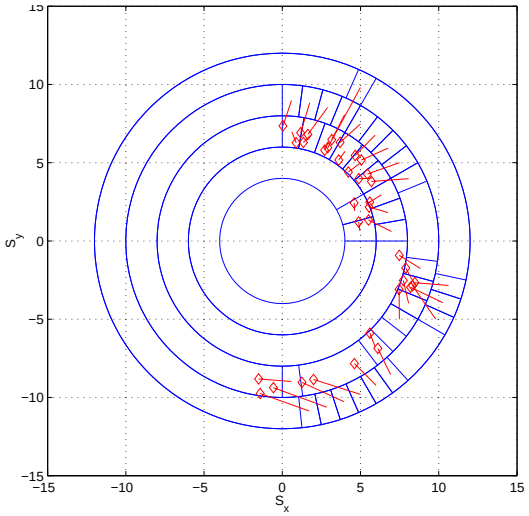

Figure 31. New SASC map for FINES.

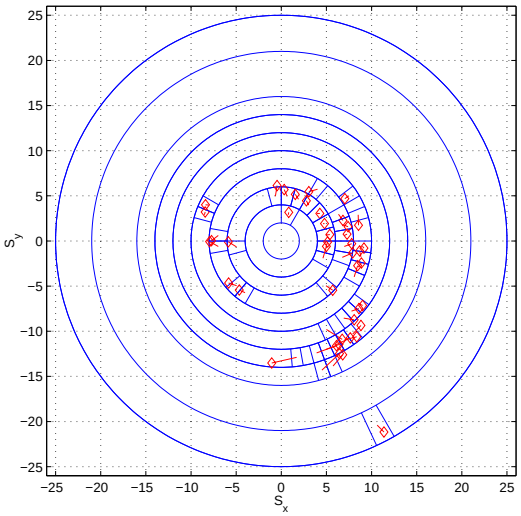

Figure 32. New SASC map for GERES.

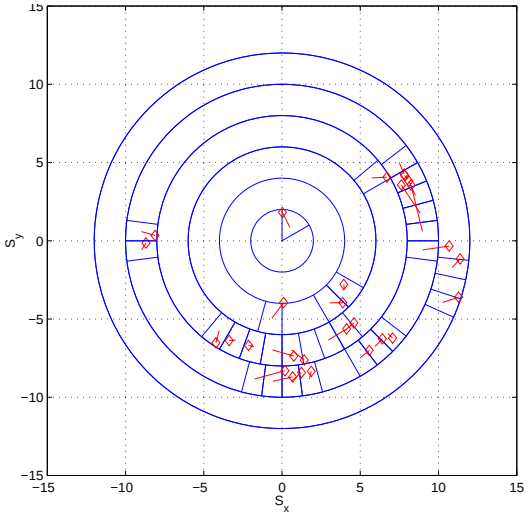

Figure 33. New SASC map for HIA.

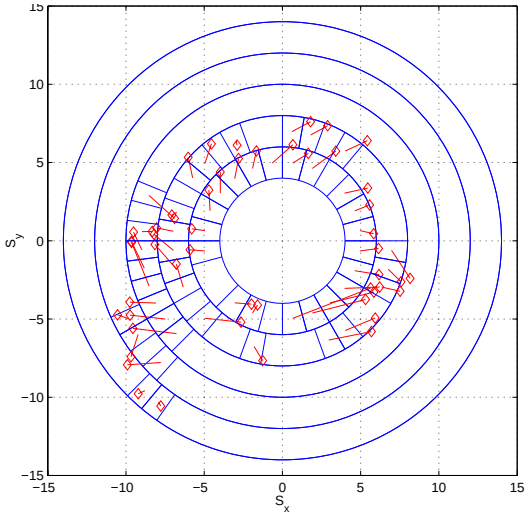

Figure 34. New SASC map for ILAR.

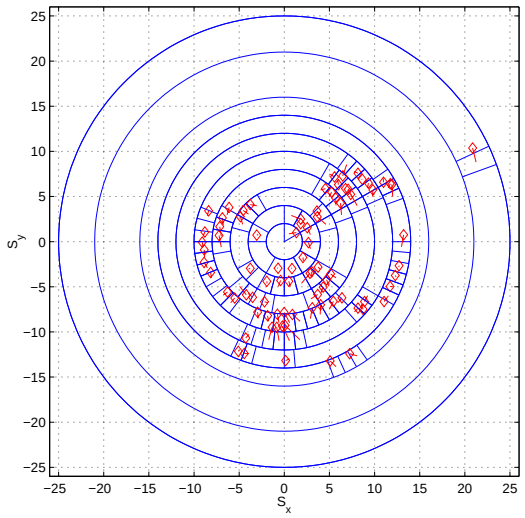

Figure 35. New SASC map for KSAR.

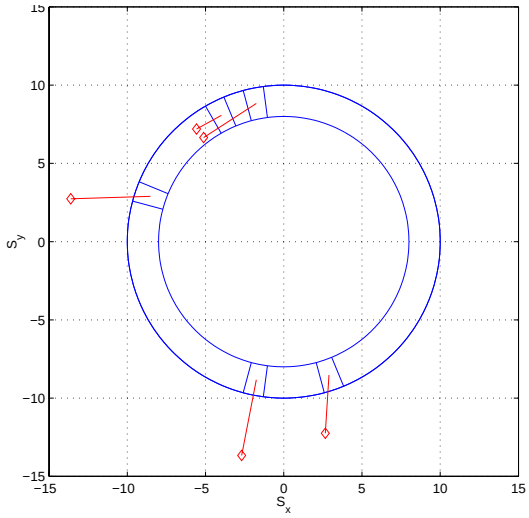

Figure 36. New SASC map for LPAZ.

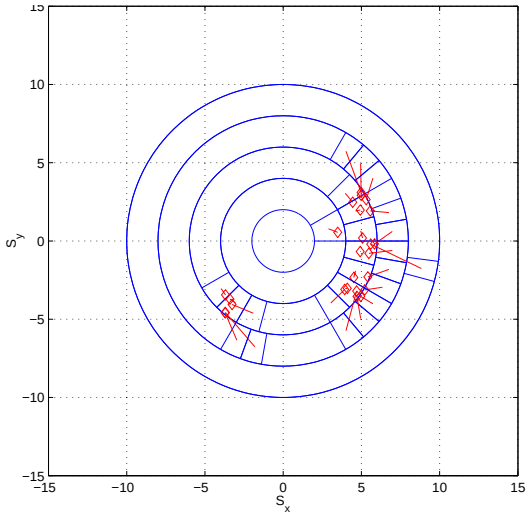

Figure 37. New SASC map for MAW.

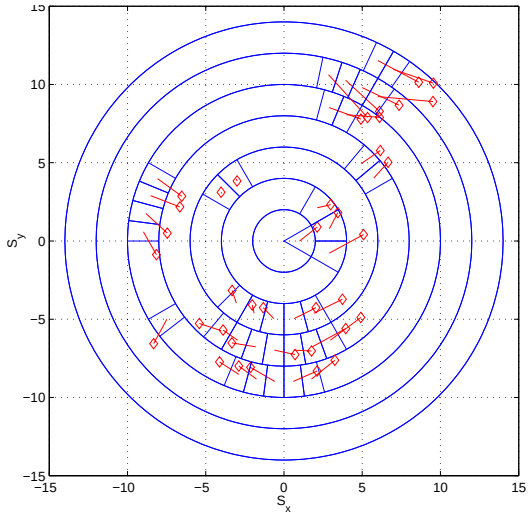

Figure 38. New SASC map for MJAR.

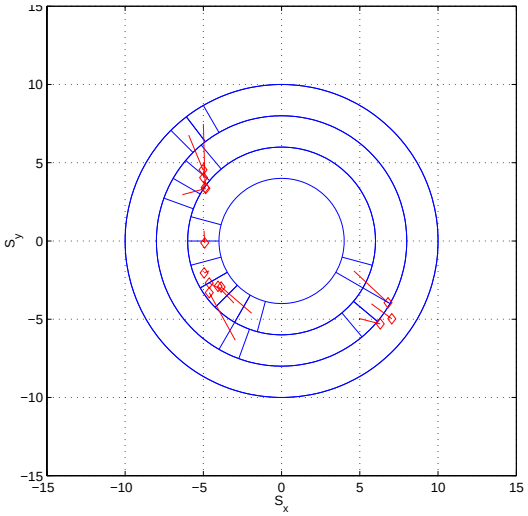

Figure 39. New SASC map for MNV.

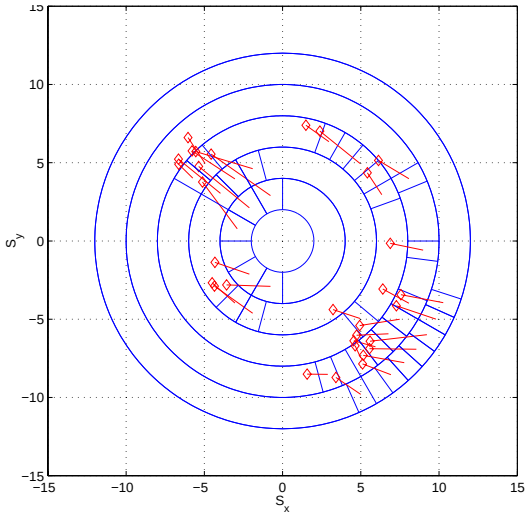

Figure 40. New SASC map for PDAR.

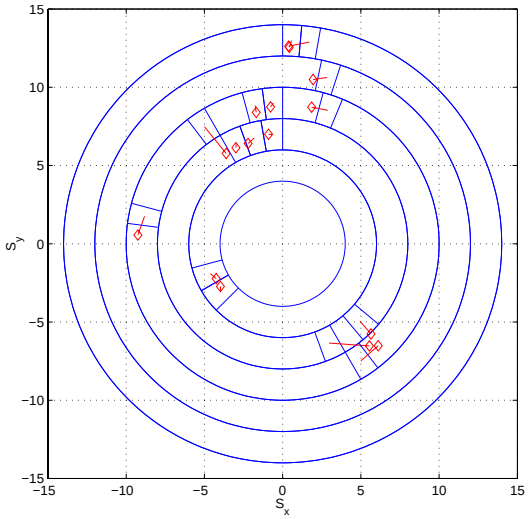

Figure 41. New SASC map for PLCA.

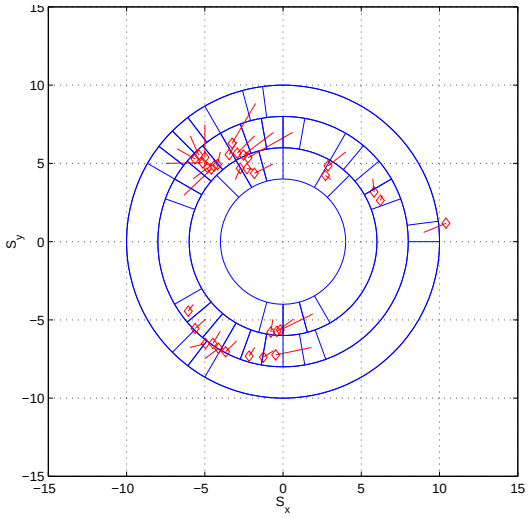

Figure 42. New SASC map for SCHQ.

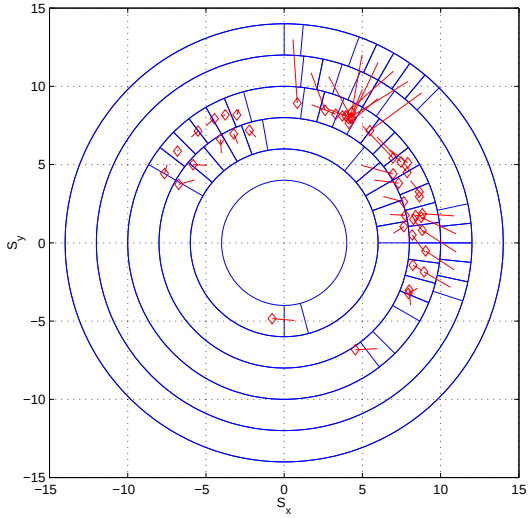

Figure 43. New SASC map for STKA.

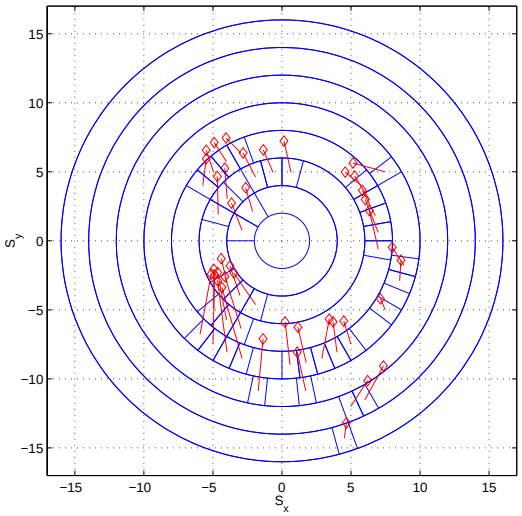

Figure 44. New SASC map for TXAR.

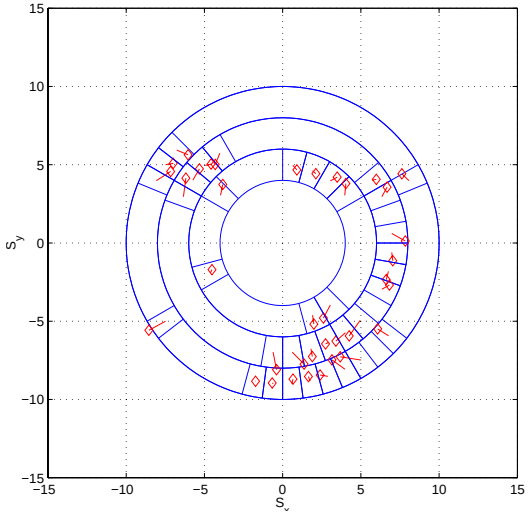

Figure 45. New SASC map for ULM.

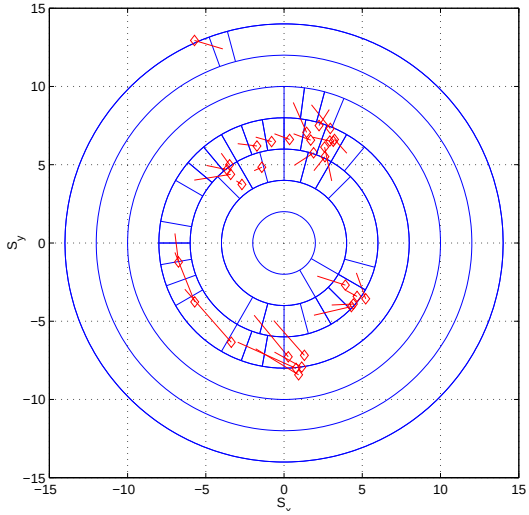

Figure 46. New SASC map for VNDA.

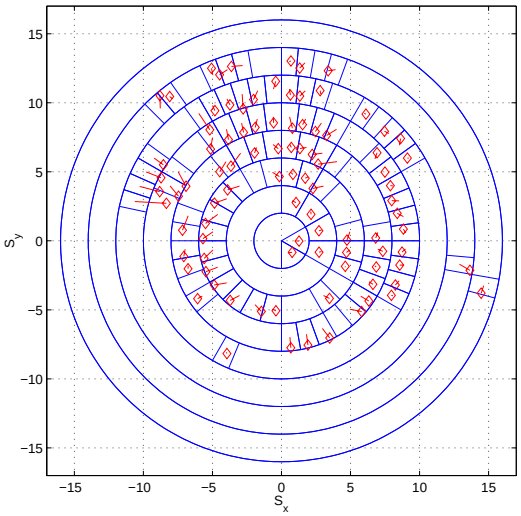

Figure 47. New SASC map for WRA.

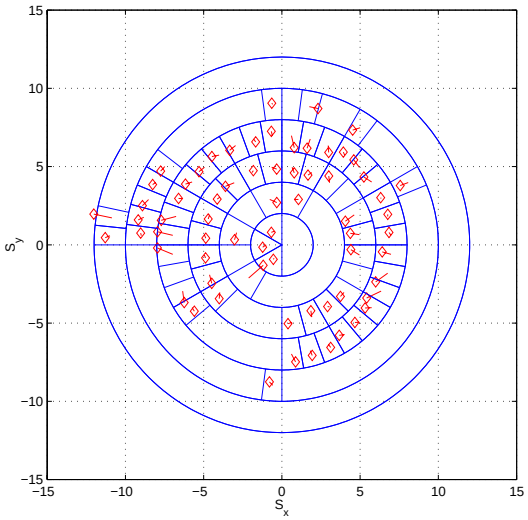

Figure 48. New SASC map for YKA.